Building and Environment 258 (2024) 111635

Contents lists available at ScienceDirect

Building and Environment

journal homepage: www.elsevier.com/locate/buildenv

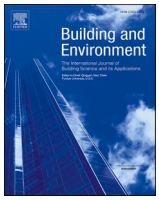

Diminishing benefits of thermal mass in Iranian climate: Present and future scenarios

Eugénio Rodrigues *, Nazanin Azimi Fereidani, Marco S. Fernandes, Adélio R. Gaspar

Univ Coimbra, ADAI, Department of Mechanical Engineering, Rua Luís Reis Santos, Pólo II, 3030-788, Coimbra, Portugal

ARTICLE INFO

Keywords:
Climate change
Overheating
Residential buildings
Thermal transmittance
Thermal mass
Iran

ABSTRACT

Thermal mass, a pivotal element in a building's performance, functions as an indoor thermal buffer. While literature underscores its advantages, the enduring impact of thermal mass amid climate change remains uncertain. This study methodically assesses thermal mass effects in 21 Iranian cities across contemporary and future climates, juxtaposing heavyweight and lightweight constructions. The EPSAP algorithm, a generative building design method, created a dataset of two-story single-family houses. Cooling and heating demands were evaluated in EnergyPlus, accounting for current and future system design efficiencies. Future climates were simulated using EC-Earth3 model estimations for the SSP5-8.5 scenario in 2050 and 2080 timeframes. The findings reveal that the energy efficiency advantage of heavyweight over lightweight buildings will diminish by up to 0.60 $kW{\cdot}h{\cdot}m^{-2}$ in 2050 (40 % less than the present-day climate difference between constructions) and 0.93 $kW{\cdot}h{\cdot}m^{-2}$ in 2080 (63 %) for cities in central and southern regions. The performance differences between constructions will sometimes be null, making thermal mass negligible. Conversely, only three cities in Northern Iran exhibit an opposing trend for mid to very-high thermal transmittances. Regarding building geometry, heavyweight construction correlates strongly with indexes related to building compactness, while lightweight construction aligns more with glazing-related indexes. However, as climates warm or we move towards warmer regions, discernible differences between lightweight and heavyweight constructions vanish for both shape- and glazing-related indexes. In conclusion, although the use of thermal mass will be less effective, building design professionals will have greater latitude for innovative construction and design solutions.

1. Introduction

Thermal mass is defined as a material's inherent ability to absorb and retain heat [1], strategically employed as a passive design measure to mitigate cooling energy demands during warmer seasons or summertime overheating in a warmer future [2]. This design choice has demonstrated notable success in stabilizing fluctuations in temperature and diminishing overall energy consumption in buildings, particularly in areas characterized by substantial daily temperature variations, resulting in considerable benefits in thermal comfort [3], as reported in the literature. For instance, a recent study concluded that increasing the thermal inertia of building walls in Poland reduced the summer's daily indoor temperature swing [4]. The same authors concluded that the thermal mass effectiveness lies in reducing temperatures closer to occupants' comfort limits, thereby diminishing the reliance on air-conditioning [5]. In the hot summer and cold winter Chinese climate zones, high thermal mass does not help reduce building loads in residential buildings; rather, it improves indoor thermal comfort control compared to low thermal mass [6]. In Indian office buildings, thermal mass can reduce excess heat discomfort for a significant time during the summer and winter seasons [7]. The decrease and stabilization of indoor daily temperatures for high-mass buildings were also observed in the hot and arid climates of Egypt [8] and Saudi Arabia [9]. In Brazil, the efficiency of thermal mass varies with the climatic conditions. It is effective in milder climates like Curitiba, enabling passive operation throughout the year. However, in more severe climates such as São Luís, buildings with high thermal mass in the envelope exhibit low thermal resilience by hindering temperature recovery [10].

The thermal response of buildings with high thermal mass is significantly more stable, helping to attenuate the daily temperature shifts [11], which, in turn, are an important factor for its effectiveness, especially when coupled with proper ventilation [12]. This factor can have a significant impact. In a study conducted during two heat waves in Poland, the authors concluded that coupling high thermal mass with

* Corresponding author.
E-mail address: erodrigues@uc.pt (E. Rodrigues).

https://doi.org/10.1016/j.buildenv.2024.111635
Received 28 January 2024; Received in revised form 9 May 2024; Accepted 11 May 2024
Available online 14 May 2024

night ventilation eliminated the hours of very high temperatures [13]. In another study, the thermal mass configuration was optimized with integrated night ventilation for different climate conditions in China. The results highlighted night ventilation's vital role in decreasing overheating even under future climate conditions [14]. While also evaluating future scenarios, natural ventilation, paired with thermal insulation and thermal mass, was the best measure to reduce future overheating in a Slovenian case study [15]. In contrast, a UK study concluded that high thermal mass paired with night ventilation is only effective in the short-term, with the ventilation effect significantly reduced in the future [16]. A study investigating buildings in five different cities in the US concluded that increasing thermal mass will increase energy savings through mixed-mode ventilation [17].

1.1. The effect of thermal mass on energy efficiency

While thermal mass is widely perceived as advantageous for maintaining optimal indoor temperatures and increasing indoor thermal comfort, the literature reveals conflicting findings on its impact on energy consumption across diverse climates. In desert climates like Australia, thermal mass significantly affects thermal behavior and reduces energy consumption, especially when positioned on the inner side of the insulation [3]. In contrast, in Las Vegas, denser construction reduced heating energy usage but increased cooling demands due to heat retention [18].

In central-western Poland's temperate climate, heavyweight construction significantly reduces the cooling energy demand during extreme heat events [13]. In Al-Ain, United Arab Emirates, the thermal mass has effectively reduced cooling and heating demands, saving up to 14.8 % in electricity consumption [19]. Similarly, in the hot semi-arid climate of Israel, high thermal mass can lower the operational energy consumption [20]. In contrast, in the tropical savannah climate of the interior of Brazil, thermal mass is employed as a strategy for cooling, greatly reducing energy consumption in residential buildings [21]. Conversely, certain studies found limited benefits [22] or no discernible advantage [11] from high thermal mass in colder climates. For example, in Canadian cities, buildings with higher thermal mass, such as those constructed with hempcrete, consumed more energy, mainly for heating [23].

Research outcomes exhibit considerable variation even within the same climatic zone. Low thermal inertia walls in Mediterranean climates heightened heating and cooling demands [24], while medium-heavy configurations exhibited lower energy consumption, particularly when paired with appropriate night ventilation [25]. However, a series of studies indicated that thermal mass, while significantly influencing comfort level, might have a modest impact on energy savings in this region [26]. It may even lead to an increase in cooling energy consumption in the southern and warmer climates while increasing the heating energy demand in northern and colder climates [27].

The impact of thermal mass on energy use appears intricately linked to variations in climate conditions. Nevertheless, discrepancies in findings also arise from different measurement standards, methodologies, simulation settings, building types, definitions of optimal thermal mass and energy usage, and a tendency to focus on specific building components rather than the entire structure [28].

1.2. The impact of thermal insulation

Previous research has disclosed that these disparities do not exclusively arise from the factors mentioned above but also stem from the intricate nature of the underlying physical phenomenon, notably the building envelope's selected thermal transmittance (*U*-value) [27]. The findings indicate that thermal transmittance exerts a varying impact on the contribution of thermal mass. For instance, within the same climate zone, exemplified by Casablanca, low thermal mass can be advantageous when coupled with higher thermal transmittance values [27]. Conversely, the relationship might be different for lower values. Therefore, the interplay between thermal mass and *U*-values significantly influences a building's energy performance. The prevailing emphasis on thick insulation mandated by energy-saving standards prompts questions about the potential benefits of combining heavyweight construction with insulation, particularly for countries with diverse climate regions.

A study in the United States underscores that while thermal insulation often surpasses the impact of thermal mass alone in reducing overall energy consumption, this dynamic shifts in hotter regions, where insulation leads to higher energy usage [29]. Adding thermal insulation generally leads to 20 %–50 % heating energy reductions, except for hot and arid climates. Meanwhile, cooling energy increases with added insulation. Interestingly, this study found that increasing insulation thickness does not consistently result in greater energy reduction, which contrasts with a previous study that added insulation diminishes the thermal benefits of mass [30]. The findings indicate that incorporating thermal insulation decreases overall energy consumption, except in hot climates. In contrast, a study in the same climate category mentions the advantages of utilizing thermal mass and insulation materials to enhance energy efficiency [20]. It means that using materials with higher thermal mass in an office building in Southern Israel could lead to a 3 % reduction in operational energy consumption, and adding insulation further decreases energy use. Another study emphasizes the significance of low thermal transmittance in regions with hot climates similar to Saudi Arabia's. It reveals that altering external walls' *U*-value (insulation level) has a more pronounced effect on energy savings than the thermal mass itself. Lowering the *U*-value reduces energy use, though the difference between high and low thermal masses is relatively small [9]. The study concludes that the *U*-value is crucial, significantly impacting wall heat flow.

Studies indicate that the insulation placement and thermal mass within walls significantly affect the energy performance of buildings. In Riyadh, a two-layered insulation configuration in the middle and on the exterior side of the wall resulted in the most substantial time lag and reduced peak loads by 20 % [31]. In comparison, exterior insulation coupled with optimal thermal mass thickness yields up to 35 % energy savings [32]. Another research work concluded that walls with thermal mass on the interior side of the wall exhibited the lowest decrement factor and minimal fluctuations in heat flux and indoor surface temperatures, contributing to energy savings [33]. Additionally, research conducted in two Palestinian climates indicated that walls with high thermal mass and high thermal insulation in the outer layer positively affected thermal performance during winter and summer, irrespective of the climate zone [34], while uninsulated walls displayed the poorest thermal performance during winter. Similarly, in the warm Mediterranean climate of Italy, the employment of a massive thermal layer on the internal side of the external wall and the resistive layer outside resulted in the optimal thermal performance solution to mitigate overheating [35]. Similar conclusions were reported for thermally massive buildings in Iran, where placing the thermal insulation on the outer side of walls results in the most efficient solution [36]. The strategic arrangement of thermal mass is essential, with some studies indicating that semi-thermal mass inside the wall (*i.e.*, thermal mass divided by the insulation layer) leads to the lowest annual heating and cooling loads, while walls with higher thermal mass concentrated on the interior side exhibited the highest energy consumption [37].

Despite a consensus on the placement of thermal mass within external walls, the effectiveness of combining this strategy with insulation still needs to be conclusive. The interaction between thermal mass and *U*-values is complex and varies with climate conditions. Moreover, the complexities introduced by climate changes underscore the need to investigate how shifts in climate might alter the interplay between thermal mass and *U*-values, influencing building energy efficiency.

Table 1 summarizes and presents the relevant literature regarding the impact of thermal mass and other related measures.

Table 1
Summary of collected literature regarding the impact of thermal mass and other related measures.

Ref.	Location	Climate[a]	Building type	Performance indicator	Results	Future climate?
[3]	Newcastle (Australia)	Humid subtropical climate	Residential	High thermal mass on the insulation' inner side	Reduction of energy consumption.	No
[4,5]	Zielona Góra (Poland)	Temperate	Residential	High thermal mass	Reduction of daily indoor temperature swing in summer.	No
[6]	Chongqing (China)	Hot Summer and Cold Winter	Residential	High thermal mass	Improvement of indoor thermal comfort control.	No
[7]	Jaipur (India)	Composite	Office	High thermal mass	Reduction of excess heat discomfort during summer and winter.	No
[8]	Cairo (Egypt)	Hot and arid	Residential	High thermal mass	Reduction and stabilization of indoor daily temperatures.	No
[9]	Riyadh (Saudi Arabia)	Hot and arid	Office	High thermal mass + thermal insulation	Reduction and stabilization of indoor daily temperatures with higher thermal mass. Added insulation has a higher impact than thermal mass.	No
[10]	Curitiba, São Luís (Brazil)	*Subtropical highland, Tropical monsoon	Residential	High thermal mass	Effective, enabling passive operation throughout the year in the milder Curitiba climate; and lower thermal resilience in the more severe São Luís climate.	No
[11]	Madrid (Spain)	Hot and dry	Office	High thermal mass	Attenuation of the daily temperature shifts.	No
[13]	Zielona Góra (Poland)	Temperate	Residential	High thermal mass + night ventilation	Elimination of hours of very high temperatures and reduction of cooling energy demand, during extreme heat.	No
[14]	Harbin, Beijing, Shanghai, Kunming, Guangzhou (China)	Severe Cold, Cold. Hot Summer Cold Winter, Temperate, Hot Summer Warm Winter	Office	Optimized thermal mass + night ventilation	Overheat reduction.	***Yes***
[15]	Ljubljana (Slovenia)	Temperate	Residential	High thermal mass + thermal insulation + natural ventilation	Overheat reduction.	***Yes***
[16]	London (UK)	*Temperate oceanic	Office	High thermal mass + night ventilation	Reduction in overheating in the short term, with the ventilation effect significantly diminished in the future.	***Yes***
[17]	Miami, Phoenix, Las Vegas, San Francisco, Philadelphia (USA)	Very hot and humid, Very hot and dry, Hot and dry, Marine climate, Warm and humid	Office	High thermal mass + mixed-mode ventilation	Higher energy savings.	No
[18]	Las Vegas (USA)	Desert climate	Residential	High thermal mass	Heating energy reduction and cooling energy increase.	No
[19]	Al-Ain (UAE)	Arid	Residential	High thermal mass	Reduction of heating and cooling demands.	***Yes***
[20]	Beer Sheva (Israel)	Hot semi-arid	Office	High thermal mass + thermal insulation	Reduction of operational energy consumption, with added adding insulation further decreasing energy use.	No
[21]	Cuiabá (Brazil)	Tropical savannah	Residential	High thermal mass	Reduction of cooling demand.	***Yes***
[22]	Växjö, Östersund, Kiruna (Sweden)	Nordic	Residential	High thermal mass	Limited impact on the heating demands.	No
[23]	Toronto, Vancouver (Canada)	Cold, Mild	Residential	High thermal mass	Higher energy consumption for heating.	No
[24]	Milan (Italy)	Continental	Residential	Low thermal mass	Higher heating and cooling demands.	No
[25]	Milan, Rome, Palermo (Italy)	*Humid subtropical, Mediterranean, Hot-summer subtropical	Office	Medium-high thermal mass + night ventilation	Lower energy consumption.	No
[26]	Ancona (Italy)	Hot-summer Mediterranean	Residential	High thermal mass	Significant impact on comfort level and modest influence on energy savings.	No
[27]	Several across the Mediterranean area	Humid subtropical, Mediterranean, Hot subtropical steppe	Residential	High thermal mass	Increase in cooling energy consumption in southern and warmer climates. Increase in heating energy demand in northern and colder climates.	No
[29]	Miami, Phoenix, San Francisco, Albuquerque, Chicago, Minneapolis, Duluth, Fairbanks (USA)	Very hot humid, Hot dry, Warm marine, Mixed dry, Cool humid, Cold humid. Very cold. Subarctic	Office	High thermal mass + thermal insulation	Thermal insulation surpasses the impact of thermal mass in reducing overall energy consumption, except in hotter regions where insulation leads to higher consumptions.	No
[30]	Phoenix, Houston, Tucson, Billings, Minneapolis, Fargo (USA)	Hot and dry, Hot and humid, Very hot, Cold and Dry, Cold and humid, Very cold	Office	High thermal mass + thermal insulation	More thermal insulation diminishes the thermal benefits of mass and decreases overall energy consumption, except in hot climates.	No
[31,32]	Riyadh (Saudi Arabia)	Hot and arid	Generic wall	Optimized thermal mass + exterior thermal insulation	Reduction of peak loads and higher energy savings.	No
[33]	Montreal (Canada); Miami, Denver (USA)	Heating-dominated, Cooling-dominated, Temperate	Office	High thermal mass on the interior side of the wall	Low decrement factor, minimal fluctuations in heat flux and indoor surface temperatures, and higher energy savings.	No
[34]	Jericho, Nabus (Palestine)	Hot dry summer and warm winter, Cold winter and hot summer	Residential	High thermal mass + thermal insulation on the outer layer	Better thermal performance during winter and summer.	No

(*continued on next page*)

Table 1 (*continued*)

Ref.	Location	Climate[a]	Building type	Performance indicator	Results	Future climate?
[35]	Lecce (Italy)	Hot Mediterranean/dry-summer subtropical	Residential	High thermal mass on the internal side + thermal insulation on the outer layer	Reduction of overheating and temperature swings	No
[36]	Shiraz (Iran)	Semi-arid	Generic wall	High thermal mass + thermal insulation on the outer layer	Higher thermal performance, with lower decrement factor and longer time lag.	No
[37]	Tehran (Iran)	Hot and arid	Residential	Thermal mass on the interior side of the wall + natural ventilation	Semi-thermal mass (massive layer divided by insulation) enhances the energy performance.	No
[38]	Santa Rosa, Mendoza, Córdoba, Orán (Argentina)	Humid subtropical, Cold desert, Monsoon-influenced humid subtropical	Residential	High thermal mass	Effectiveness reduction of thermal mass in the future in certain locations.	***Yes***

[a] Climate classification according to the respective research work, except where missing (marked with *), for which the Köppen-Geiger climate classification [39] was considered here.

1.3. Future weather

Given the current context of climate change, a few studies stress the importance of thermal mass evaluation under future climate (Table 2), with some future projections suggesting a potential decrease in the thermal mass strategy's effectiveness in certain locations [38]. These studies employ future weather data to simulate future buildings' performance, but most of them use outdated climate data from the HadCM3 model produced for CMIP2 experiments [40], which date from 2001 and were the basis for the 4th assessment report of The Intergovernmental Panel on Climate Change (IPCC). The future climate scenarios from these experiments are much less detailed than the ones in the recent 6th assessment report of the IPCC, the Shared Socioeconomic Pathways (SSP). Other issues must be pointed out, such as the coarse spatial resolution of the climate data and the tools that implement the morphing procedure (CCWorldWeatherGen and Weather Morph), lack of statistical transforming of all variables needed in the dynamic simulation of buildings and interpolation method of the data to the location of the building [41]. The remaining studies use Meteonorm data or transformation of design summer year with a probabilistic prediction of climate change, which, from 2009, uses an old climate scenario, and the second study only accounts for summer overheating. Therefore, there is a clear lack of knowledge on the role of thermal mass under climate change scenarios, both due to the small number of studies that only cover a small number of locations worldwide and the use of outdated climate data.

1.4. The Iranian context

The building sector in Iran faces significant challenges, particularly in terms of energy consumption and thermal efficiency. A major portion of Iran's energy consumption is attributed to buildings, with approximately 40 % of the total energy used for heating and cooling [42]. This high energy consumption is exacerbated by the country's status as the world's leading source of energy subsidies in 2020 [43]. The availability of these subsidies and economic assistance from the Iranian government in the building energy industry has diminished the emphasis on energy efficiency in building envelopes [43]. Consequently, thermally efficient exterior walls are not commonly found in Iranian buildings, and selecting exterior wall materials often disregards appropriate criteria [43]. This disregard for thermal efficiency poses significant challenges, especially given the ongoing climate warming trend. Projections suggest that the mean annual temperature in Iran is anticipated to rise by approximately 5.2 °C by the end of the century [44]. This situation will likely exacerbate without intervention, making buildings increasingly inefficient and energy-intensive.

Research on the influence of thermal mass on building energy efficiency in Iran remains sparse. While recent studies have emphasized its significant impact on thermal performance across various climates, most have predominantly focused on the placement of thermal insulation within conventional wall types [43] or optimizing the thickness of thermal insulation [45]. There is a notable gap when considering alterations to wall mass.

Researchers who have investigated the impact of thermal mass in Iran have primarily focused on positioning thermal mass within walls to determine where it can yield optimal thermal performance [36,37], as discussed in the preceding section. Some studies have also assessed the combination of thermal mass with other strategies. For instance, it was discovered that cases with higher thermal mass, such as 25 cm high-density concrete blocks or 30 cm outer bricks in external walls, along with additional layers of insulation positioned externally, could significantly enhance building performance in a school building during the winter season in the arid, steppe, cold climate of Tehran [46]. In another study, by increasing the thermal mass, particularly using concrete structures and interior brick walls, in buildings constructed with straw bale material, substantial reductions in energy consumption were

Table 2
Studies focusing on the evaluation of thermal mass under climate change.

Ref.	Location	Timeframe	Scenario	Model	Tool	Performance indicator
[14]	Harbin, Beijing, Shanghai, Kunming, Guangzhou (China)	2050, 2080	A1FI (High emissions), A2 (Medium-high emissions), B1 (Medium-low emissions), B2 (Low emissions)	HadCM3	Weather Morph	Comparison of overheating hours between different timeframes, scenarios, and construction types, with and without night ventilation.
[15]	Ljubljana (Slovenia)	2011–2040, 2041–2070, 2071–2100	A2 (Medium-high emissions)	HadCM3	CCWorldWeatherGen	Effect of overheating-preventing measures (*e.g.*, thermal mass, ventilation) on the operative temperature and thermal comfort for the different timeframes.
[16]	London (UK)	1970, 2030, 2050, 2080	Medium emissions, High emissions	–	DSY weather file with probabilistic prediction for climate change	Effect of high thermal mass on the overheating hours, for the different timeframes and scenarios, and for different ventilation rates.
[19]	Al-Ain (UAE)	Present, 2050, 2100	Scenario-1 (+1.6 °C in 2050), Scenario-2 (+2.3 °C in 2100), Scenario-3 (+2.9 °C in 2050), scenario-4 (+5.9 °C in 2100)	–	MeteoNorm	Comparison of energy demand and CO_2 emissions for the different timeframes and scenarios with distinct design measures (*e.g.*, thermal mass, insulation, shading).
[21]	Cuiabá (Brazil)	1961–1990, 2011–2040, 2041–2070	A2 (Medium-high emissions)	HadCM3	CCWorldWeatherGen	Comparison of energy consumption, cooling degree-hours, operative temperatures, and discomfort hours for the different timeframes and construction types, and for different orientations.
[38]	Santa Rosa, Mendoza, Córdoba, Orán (Argentina)	1961–1990, 2020, 2050, 2080	A2 (Medium-high emissions)	HadCM3	CCWorldWeatherGen	Comparison of temperature of thermal neutrality and energy consumption for the different timeframes, with distinct passive strategies (*e.g.*, thermal mass, natural ventilation, shading).

observed across all climates of Iran. However, the extent of improvement varied among locations, with some areas such as Yazd (arid, desert, hot) and Rasht (temperate, no dry season, hot summer) necessitating higher thermal mass for optimal performance [47]. Conversely, in another study utilizing Givoni's correction chart to provide bioclimatic recommendations across ten climates in Iran, the use of high thermal mass was only recommended for Abadan, a city characterized by a hot-desert climate, for both present and future time frames [48]. Therefore, the literature on this topic in Iran is limited, with findings often exhibiting inconsistent results across different climates in Iran.

1.5. Aim and contributions

Despite the existent literature stressing the importance of thermal mass on energy efficiency, thermal resilience, and the impact of distinct factors (*e.g.*, ventilation, thermal insulation, climatic context), there are limited works addressing the optimal interplay between thermal mass and thermal transmittance amidst climate change. In addition, such topics are rarely investigated in the context of Iran, with few existing studies addressing them separately (as mentioned in Section 1.4). Our research aims to fill this void by exploring such relationships and their impact on building energy performance. This study addresses three key questions: "Will thermal mass remain effective in the future?", "How do variations in *U*-values and climate impact the role of thermal mass in buildings?" and "Will thermal mass affect the building geometry options?"

This study takes a distinctive and novel approach that uses a generative design method to produce large synthetic datasets comprising detailed single-family homes across multiple Iranian locations with varying degrees of thermal mass construction, incorporating randomized values for thermal transmittance in building envelope components. Their energy performance is determined using dynamic simulation under current and future climate scenarios, which were morphed using the most recent climate data from the latest Assessment Report of the IPCC and statistically analyzed to determine their trend over time and identify the most important design aspects.

This work provides new insights by presenting representative findings on the relation between thermal mass and thermal transmittance while accounting for the effect of climate change. It contributes to the body of knowledge by referencing similar buildings and climates where comparably significant findings are lacking. The results of this research may also help building professionals employ the best strategies in the face of climate change.

The remaining paper is structured in four additional sections. In Section 2, the material and methods employed in this study are described and justified. The results are presented in Section 3 and are discussed in Section 4. Finally, the conclusions are made in Section 5.

2. Materials and methods

We followed a systematic approach to address the hypothesis that climate change will impact the role of thermal mass in buildings, which affects both energy performance and geometry design options, as outlined below in six steps. Fig. 1 provides a visual illustration of our study concept framework.

Step 1. In the initial stage, we obtained typical meteorological weather data for Iran from the climate.onebuilding.org website. We assessed the integrity of this weather data (derived from historical records from 2004 to 2018). This dataset served as our representation of the present-day climate.
Step 2. The present-day climate data underwent statistical transformation to create a future climate scenario (SSP5-8.5) for two specific timeframes, namely 2050 and 2080. We achieved this transformation using the Future Weather Generator morphing tool. The present-day and future climates were utilized to define outdoor conditions in Step 4.
Step 3. Subsequently, we generated alternative designs for a two-story single-family house using the generative design technique known as the EPSAP algorithm. This process resulted in 115,200 distinct building designs.
Step 4. EnergyPlus simulated the buildings' energy performance with randomized window, wall, and roof thermal transmittances for each thermal mass construction (heavyweight and lightweight). Two hundred thirty-four hundred simulations were carried out for each location and climate timeframe.
Step 5. We organized the simulation results into two datasets, one for heavyweight construction and another for lightweight. Within these

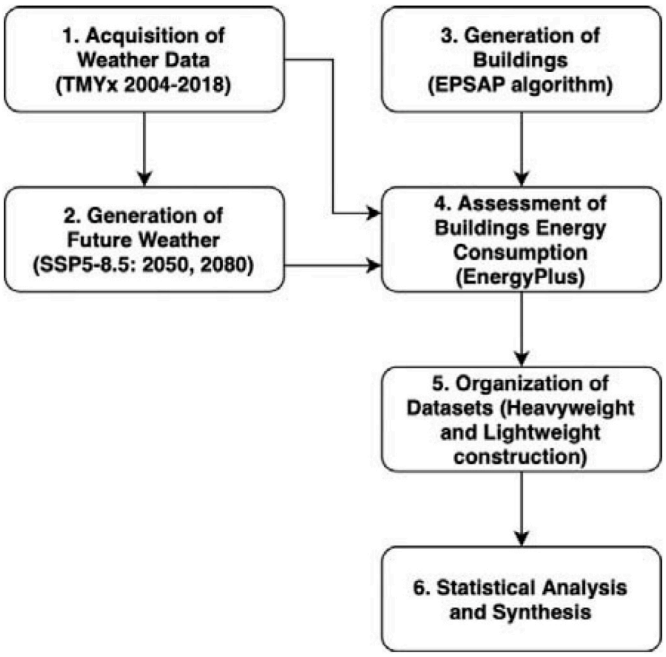

Fig. 1. Study concept framework.

datasets, we calculated the cooling and heating energy consumption in conditioned zones, considering the anticipated efficiencies of the Heating, Ventilation, and Air Conditioning (HVAC) system corresponding to the chosen climate scenario.

Step 6. Finally, we conducted a comprehensive statistical analysis and comparative assessment of the two datasets to synthesize our findings. This analysis involved leveraging information about energy performance, construction properties, and building geometry to discern statistical relationships and identify trends over time.

The study involved 14,515,200 simulations, considering various building geometries, locations, climate timeframes, and thermophysical properties. The following sections describe in detail the materials and methods used.

2.1. Present-day and future climates

The study analyzes the role of thermal mass in twenty-one locations. These locations encompass a diverse range of climate types found in Iran according to Köppen-Geiger climate classification [39], including arid, desert, hot (BWh), arid, steppe, hot (BSh), arid, desert, cold (BWk), arid, steppe, cold (BSk), hot-summer Mediterranean (Csa), humid subtropical (Cfa), and humid continental (Dsa) climates.

The selected locations include cities along the Caspian Sea coastline (Rasht, Ramsar, Nowshahr, and Sari), the Persian Gulf coastline (Bandar Mahshahr, Bandar Bushehr, Dayyer, Assaluyeh, Bandar Abaass, Bandar Lengeh, and Chabahar), as well as inland cities (Tabriz, Karaj, Hamedan, Tehran, Semnan, Kashan, Yazd Sadooghi, Shiraz, Sirjan, and Fasa). Further geographical and climatic information for these locations is provided in Table 3. The selection of these locations follows criteria presented in a previous study [49].

For the present-day climate, 21st-century hourly weather was retrieved from the climate.onebuilding.org website [50] and is derived from meteorological records between 2004 and 2018 following the ISO 15927–4:2005 standard [51].

Relatively to the future weather data, it was synthetically produced by morphing the present-day weather data to match a chosen projected scenario. The Future Weather Generator was used [52]. The tool was developed using climate data from one of the latest general circulation models, and it addresses several issues found in other weather morphing tools [41].

The climate data used in this study originated from the EC-Earth3 model, as detailed in Döscher et al. [53], and was a crucial component in the CMIP6 (Coupled Model Intercomparison Project Phase 6) experiments [54], forming the basis for the 2022 IPCC's 6th Assessment Report. The EC-Earth3 climate system is a comprehensive model encompassing various physical domains and system components, each playing a vital role in simulating Earth's climate dynamics. These domains and components include the atmosphere, ocean, sea ice, land surface, dynamic vegetation, atmospheric composition, ocean biogeochemistry, and the Greenland Ice Sheet [53]. The EC-Earth3 model operates on a grid with an 80 km atmospheric resolution (T255L91) and a 1.0° ocean resolution (ORCA1L75).

For validation purposes, the performance of the EC-Earth3 model has been assessed in previous studies, providing confidence in its ability to simulate real-world climate phenomena. References to these validation studies can be found in Refs. [55,56].

Table 3
Geographic data and climate classification adapted from Ref. [49].

Location				Climate	
City	Lat. (°)	Long. (°)	Alt. (m)	Type	Description
Tabriz	38.13° N	46.23° E	1359	BSk	Arid, steppe, cold
Rasht	37.32° N	49.60° E	−12	Cfa	Temperate, no dry season, hot summer
Ramsar	36.91° N	50.68° E	−21	Csa	Temperate, dry summer, hot summer
Nowshahr	36.65° N	51.50° E	−21	Csa	Temperate, dry summer, hot summer
Sari	36.63° N	53.19° E	10	BSh	Arid, steppe, hot
Karaj	35.77° N	50.82° E	1271	BSk	Arid, steppe, cold
Hamedan	34.85° N	48.53° E	1749	BSk	Arid, steppe, cold
Tehran	35.68° N	51.31° E	1207	BSk	Arid, steppe, cold
Semnan	35.59° N	53.49° E	1117	BWk	Arid, desert, cold
Kashan	33.89° N	51.57° E	1056	BWh	Arid, desert, hot
Yazd Sadooghi	31.90° N	54.27° E	1235	BWh	Arid, desert, hot
Shiraz	29.53° N	52.58° E	1499	BSh	Arid, steppe, hot
Sirjan	29.46° N	55.71° E	1739	BSk	Arid, steppe, cold
Fasa	28.89° N	53.72° E	1298	BSh	Arid, steppe, hot
Bandar Mahshahr	30.55° N	49.15° E	2	BWh	Arid, desert, hot
Bandar Bushehr	28.94° N	50.83° E	20	BSh	Arid, steppe, hot
Dayyer	27.83° N	51.93° E	4	BWh	Arid, desert, hot
Assaluyeh	27.36° N	52.73° E	8	BWh	Arid, desert, hot
Bandar Abass	27.21° N	56.37° E	6	BWh	Arid, desert, hot
Bandar Lengeh	26.53° N	54.82° E	20	BWh	Arid, desert, hot
Chabahar	25.28° N	60.61° E	8	BWh	Arid, desert, hot

Our study employed the SSP5-8.5 scenario to project future climate conditions. This scenario anticipates a substantial increase in current CO_2 emissions, nearly doubling by 2050, leading to a significant rise in the average global temperature of approximately 4.3 °C by 2100. While it may not be the most probable scenario, SSP5-8.5 is considered the most impactful, and numerous researchers deem its study [57].

Monthly changes from the current climate to the SSP5-8.5 scenario are computed from each median month of the present-day period (1985–2014) and the two future timeframes—2050 (2036–2065) and 2080 (2066–2095). The monthly changes for each variable are spatially downscaled using the bilinear interpolation method and the four nearest points of the grid to the weather data's location. Further information about the tool and the method formulation may be found on the tool's website [58].

2.2. Building geometry generation

The building geometries in this study were produced using the EPSAP algorithm [59], a generative design method. EPSAP is a population-based hybrid evolution strategy that uses a stochastic hill-climbing method instead of the traditional mutation and crossover operators. Each candidate design has its geometry and topology transformed and kept if the produced result is better or equal to the pre-transformed design. The transformations comprise the translation, reflection, rotation, stretching, and alignment of a single space to a cluster of spaces.

The algorithm determines if the transformation leads to an improved solution by minimizing a weighted-sum cost function of seventeen penalty functions. These penalty functions evaluate (i) the building's maximum gross and construction areas, compactness, and circulation areas, (ii) the overflow, connectivity, overlapping, fixed position, minimum dimensions, and relative importance of the zones, and (iii) the accessibility, minimum dimensions, overlapping, orientation, and fixed position of the openings. Further methodological detail on this algorithm may be found in Refs. [60,61] and its validation in Ref. [62].

The EPSAP algorithm generates diverse designs while adhering to a common functional program. This program encompasses the indoor arrangement of rooms and openings in the building. These designs must meet specific constraints, including minimum and maximum dimensional requirements for rooms, windows, and doors, as well as topological specifications that dictate the relationships between rooms and the orientation of elements. In essence, despite variations in volume, floor area, window-to-wall ratio, orientation, compactness, and indoor layout, all resulting building designs maintain the integrity of the predefined functional program.

The functional program is a two-story single-family house used in a previous study [49]. The functional program consists of two floors interconnected by a staircase. The ground floor comprises a hall, a living room, a kitchen, and a bathroom. On the second floor, a corridor connects three bedrooms and a second bathroom. Table 4 depicts all requirements and preferences for zones and openings used in this study.

Table 4
Functional program requirements and preferences for zones and openings. Based on Ref. [49].

Zone	C^{sn}	C^{sf}	C^{ri}	C^{sl}	C^{su}	C^{ss} (m)	C^{sa} (m^2)	C^{ssr} (−)	C^{slr} (−)
S_1	Hall	Circulation	Min	L_1	L_1	2.70	10.0	{2.0, 3.0}	{3.0, 1.5}
S_2	Living room	Living	Max	L_1	L_1	3.20	–	1.7	2.0
S_3	Kitchen	Service	Mid	L_1	L_1	1.80	–	1.7	2.0
S_4	Bathroom	Service	Min	L_1	L_1	2.20	–	1.7	2.0
S_5	Stair	Circulation	–	L_1	L_2	–	–	–	–
S_6	Corridor	Circulation	None	L_2	L_2	1.40	6.0	{2.0, 3.0}	{3.0, 1.5}
S_7	Double bedroom	Living	High	L_2	L_2	2.70	–	1.7	2.0
S_8	Double bedroom	Living	High	L_2	L_2	2.70	–	1.7	2.0
S_9	Single bedroom	Living	Mid	L_2	L_2	2.70	–	1.7	2.0
S_{10}	Bathroom	Service	Min	L_2	L_2	2.20	–	1.7	2.0

Exterior Opening	C^{os}	C^{oet}	C^{oew}(m)	C^{oeh} (m)	C^{oev} (m)
Oe_1	S_1	Door	1.00	2.00	0
Oe_2	S_2	Window	2.80	2.00	0
Oe_3	S_3	Window	1.20	1.00	1.00
Oe_4	S_4	Window	0.60	0.60	1.40
Oe_5	S_5	Window	0.80	1.40	0.80
–	S_6	–	–	–	–
Oe_6	S_7	Window	1.80	1.00	1.00
Oe_7	S_8	Window	1.80	1.00	1.00
Oe_8	S_9	Window	1.20	1.00	1.00
–	S_{10}	–	–	–	–

Interior Opening	C^{oit}	C^{oia}	C^{oib}	C^{oiw} (m)	C^{oih} (m)	C^{oiv} (m)
Oi_1	Door	S_1	S_2	0.90	2.00	0
Oi_2	Door	S_1	S_3	0.90	2.00	0
Oi_3	Door	S_1	S_4	0.90	2.00	0
Oi_4	Door	S_5	S_1	0.90	2.00	0
Oi_5	Adj.	S_2	S_3	0	–	–
Oi_6	Door	S_5	S_6	0.90	2.00	0
Oi_7	Door	S_6	S_7	0.90	2.00	0
Oi_8	Door	S_6	S_8	0.90	2.00	0
Oi_9	Door	S_6	S_9	0.90	2.00	0
Oi_{10}	Door	S_6	S_{10}	0.90	2.00	0

C^{sn} – name, C^{sf} – function, C^{ri} – relative importance, C^{sl} and C^{su} – served lower and upper stories, C^{ss} – minimum side, C^{sa} – minimum area, C^{ssr} and C^{slr} – zone smaller and larger side ratios, L_1 and L_2 – story 1 and 2.
C^{os} – zone, C^{oet} – opening type, C^{oew} – width, C^{oeh} – height, C^{oev} – vertical position.
C^{oit} – type, C^{oia} and C^{oib} – connecting zones, C^{oiw} – width, C^{oih} – height, C^{oiv} – vertical position, Adj. – adjacency.

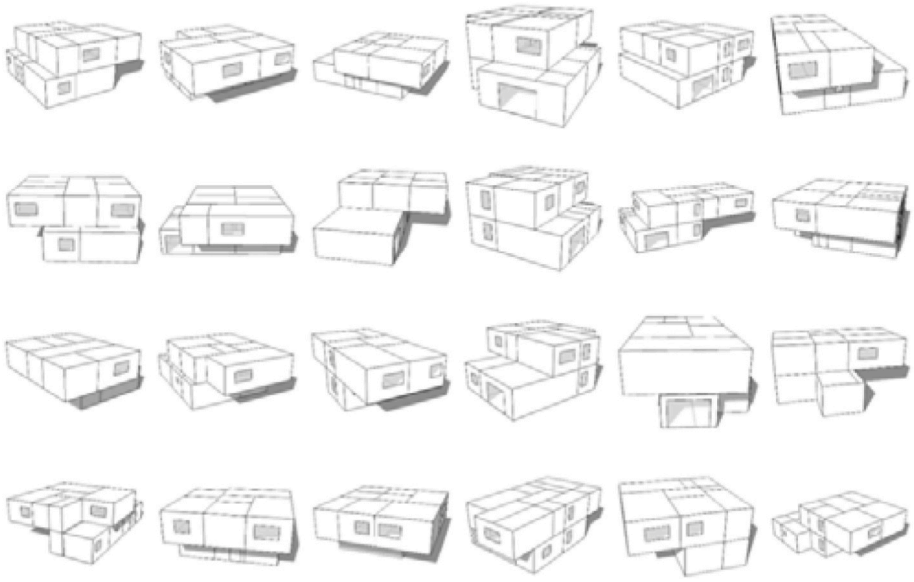

Fig. 2. Examples of the generated building geometries (from Ref. [49]).

Fig. 2 illustrates building geometries generated with different volumes, orientations, and floor plan arrangements.

2.3. Building performance simulation

The energy performance evaluation of each building within the dataset was carried out using EnergyPlus version 23.1 through a multizone annual simulation. This simulation process is integrated with the EPSAP algorithm and occurs after the building generation procedure [63]. For these simulations, a time step of 15 min was chosen, and the results are primarily focused on assessing the building's energy consumption in the air-conditioned spaces.

Subsequent sections elaborate on further details regarding the internal gains, HVAC systems, airflow patterns, and construction specifications utilized in these simulations.

2.3.1. Internal gains specifications

The internal gains considered in the simulations represent a generic single-family house accommodating five occupants. These gains follow the expected occupancy, lighting, and equipment activities in each zone (Table 5). The schedules are presented in Fig. 3.

Furthermore, daylighting control mechanisms are implemented to optimize energy efficiency. These controls include dimming the artificial lighting with the SplitFlux method in zones with exterior windows and automatically turning off artificial lights when natural sunlight exceeds an illumination level of 300 lux. Each zone has a dimming reference point located at the geometric center of each zone, which is 0.8 m from the floor. Window shades are closed during nighttime to minimize energy consumption and provide privacy and safety.

For more comprehensive information on these parameters, including the occupancy and operating schedules, please refer to the details provided in Ref. [64].

2.3.2. HVAC and airflow specifications

In this study, the living room and the bedrooms are the only rooms with heating and cooling, with the system's availability depending on the occupancy in each room. The HVAC template zone ideal loads air system is used, and the temperature thermostat setpoints for heating and cooling are 20 °C and 25 °C, respectively, according to the Iranian Building Code [65]. This system meets the thermal energy needs for the living room and bedrooms, assuming 100 % efficiency and using a generic primary energy source. The choice of an ideal system serves two purposes: (a) it simplifies the system's definition, given the uncertainty about future HVAC equipment, and (b) it facilitates the consideration of various future system efficiencies to calculate the impact of primary energy consumption (which is treated as electric energy in this study).

Currently, the seasonal coefficient of performance (SCOP) stands at 2.11 for heating and 3.35 for cooling, which are the averages from real data. It is important to note that efficiency is expected to increase. According to existing literature [66–68], it is projected that the efficiency of electric heating and cooling systems will improve by the year 2100, reaching a value of 3.875 under the SSP5-8.5 scenario. Hence, for both the current SCOP values (baseline) and the anticipated values in 2100, a straightforward interpolation yields 2.77 and 3.55 in 2050 and 3.43 and 3.74 in 2080 for heating and cooling SCOP, respectively.

Mechanical ventilation is considered to have a 0.6 h^{-1} air change exhaust rate during occupancy in the kitchen and bathrooms. Additional 0.2 h^{-1} and 0.1 h^{-1} air changes are defined for the outdoor air

Table 5
Occupancy, lighting, and equipment specifications in each zone. Based on Ref. [64].

Zone type	Occupancy		Electric lighting	Electric equipment
	Max. number of people[a]	Activity level (W·person^{-1})	Design level (W·m^{-2})	Design level (W)
Living room	5	110	7.5	350
Bathrooms	1	207	7.5	100
Circulation areas	1	190	3.2	20
Kitchen	2	190	5.0	1440
Double bedrooms	2	72	7.5	250
Single bedroom	1	72	7.5	250

[a] Number of dwellers accessing each zone and not necessarily the number of occupants simultaneously in the zone. The occupants' distribution is defined together with the proper occupancy schedules.

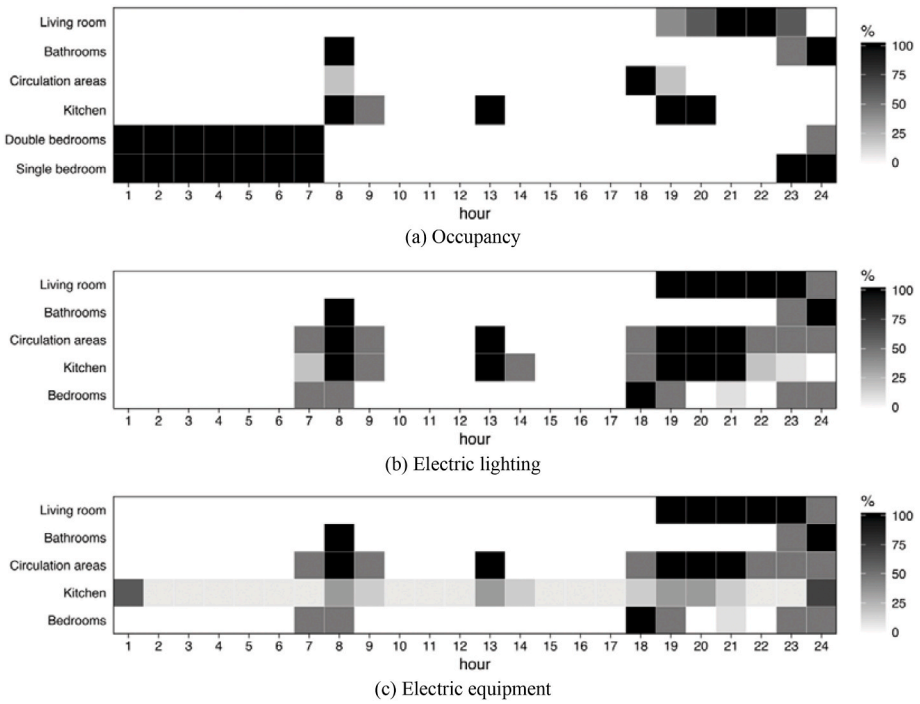

Fig. 3. Occupancy, lighting, and equipment use schedules in each zone. Based on Ref. [64].

infiltration in zones with and without exterior openings, respectively.

2.3.3. Construction specifications

For each thermal mass level to be studied, and given the nature of this research, the exterior opaque elements of the building exhibit similar thermal mass and are assigned random triple-wise values for thermal transmittances. Consequently, it becomes impractical to establish their dynamic characteristics, thereby hindering the comprehensive utilization of the admittance method outlined in ISO 13786:2017 [69]. As a result, thermal mass (expressed in $kg{\cdot}m^{-2}$) is employed as a simplified representation of the thermal inertia's impact, with heavyweight construction corresponding to high thermal mass values and lightweight construction to low thermal mass values.

The exterior window, wall, and roof thermal transmittances set a triplet. The window value varies from 0.2 $W{\cdot}m^{-2}{\cdot}K^{-1}$ to 5.0 $W{\cdot}m^{-2}{\cdot}K^{-1}$ in steps of 0.1 $W{\cdot}m^{-2}{\cdot}K^{-1}$, the wall value between 0.05 $W{\cdot}m^{-2}{\cdot}K^{-1}$ and 1.25 $W{\cdot}m^{-2}{\cdot}K^{-1}$ in steps of 0.05 $W{\cdot}m^{-2}{\cdot}K^{-1}$, and the roof value ranges from 0.05 $W{\cdot}m^{-2}{\cdot}K^{-1}$ to 1.01 $W{\cdot}m^{-2}{\cdot}K^{-1}$ in steps of 0.04 $W{\cdot}m^{-2}{\cdot}K^{-1}$. The values vary proportionally in a triple-wise fashion. In other words, the scale of thermal transmittances begins with the triplet {0.2 $W{\cdot}m^{-2}{\cdot}K^{-1}$, 0.05 $W{\cdot}m^{-2}{\cdot}K^{-1}$, 0.05 $W{\cdot}m^{-2}{\cdot}K^{-1}$} and ends with the triplet {5.0 $W{\cdot}m^{-2}{\cdot}K^{-1}$, 1.25 $W{\cdot}m^{-2}{\cdot}K^{-1}$, 1.01 $W{\cdot}m^{-2}{\cdot}K^{-1}$}. The triplets of *U*-values follow the tendency of real cases, where the *U*-values of windows, walls, and roofs decrease or increase proportionally. Table 6 lists the intervals and thermophysical properties of these elements.

The thermal mass of the exterior opaque elements is equivalent to that of the interior slab. Solar absorptance of 0.75 was used for all outer surfaces. Although the windows' solar heat gain coefficient also tends to vary according to the window *U*-value, a fixed 0.6 was chosen to capture only the impact of thermal transmittance variation. A visible transmittance (VT) value of 0.6 was used.

The ground floor and interior door constructions are similar in both levels of thermal mass, and their thermophysical properties are presented in Table 7.

Table 8 and Table 9 present the elements that have their thermophysical properties fixed, such as interior walls and interior slabs, but are different according to the thermal mass level for heavyweight and lightweight construction, respectively.

2.4. Comparison analysis and synthesis

Two buildings' geometry, construction, and performance datasets were created—one for each thermal mass level—containing the results for the present-day, 2050, and 2080 timeframes. A statistical analysis was conducted by splitting each dataset into clusters according to the thermal transmittance values of their envelope elements (25 triplets of *U*-values for windows, walls, and roofs).

The relative energy intensity differences between heavyweight and lightweight constructions were calculated in relative terms (%)—a percentage of the energy intensity difference concerning energy intensity found for the lightweight construction—for each timeframe: present day, 2050, and 2080. Thus, a negative percentage means heavyweight construction has a lower energy intensity than lightweight construction. Similarly, but presenting absolute energy intensity difference values (Δ $kW{\cdot}h{\cdot}m^{-2}$), cooling and heating consumptions are calculated.

Afterward, the Coefficient of Determination (R^2) of each triplet for five geometry indexes was computed, and the differences between their

Table 6
Thermophysical properties of the building elements that are random. Based on Ref. [64].

Element	*U* ($W{\cdot}m^{-2}{\cdot}K^{-1}$)	Mass ($kg{\cdot}m^{-2}$)	α (–)	SHGC (–)	VT (–)
Exterior wall	RAND {0.05, …, 1.25}	Equivalent to the mass of the interior slab.	0.75	–	–
Roof	RAND {0.05, …, 1.01}	Equivalent to the mass of the interior slab.	0.75	–	–
Exterior window	RAND {0.2, …, 5.0}	–	–	0.6	0.6

U – thermal transmittance, α – solar absorptance, SHGC – solar heat gain coefficient, VT – visible transmittance.

Table 7
Thermophysical properties of the building elements common to both construction types that are fixed. Based on Ref. [27].

Element	Layer	Thick. (m)	k (W·m^{-1}·K^{-1})	ρ (kg·m^{-3})	c_p (J·kg^{-1}·K^{-1})	U (W·m^{-2}·K^{-1})	Mass (kg·m^{-2})
Ground floor	Structural layer	0.200	1.730	2245.6	836.8	0.437	509.69
	Insulation layer	0.080	0.040	32.1	836.8		
	Filling layer	0.020	0.800	1600.0	840.0		
	Regulation layer	0.010	0.220	950.0	840.0		
	Finishing layer	0.020	0.200	825.0	2385.0		
Interior door	Finishing layer	0.005	0.200	825.0	2385.0	2.009	21.15
	Structural layer	0.030	0.067	430.0	1260.0		
	Finishing layer	0.005	0.200	825.0	2385.0		

k – thermal conductivity, ρ – density, c_p – specific heat, U – thermal transmittance.

Table 8
Thermophysical properties of the building elements for the heavyweight construction that are fixed. Based on Ref. [27].

Element	Layer	Thick. (m)	k (W·m^{-1}·K^{-1})	ρ (kg·m^{-3})	c_p (J·kg^{-1}·K^{-1})	U (W·m^{-2}·K^{-1})	Mass (kg·m^{-2})
Interior wall	Finishing layer	0.020	0.220	950.0	840.0	4.499	195.01
	Structural layer	0.070	1.730	2243.0	836.8		
	Finishing layer	0.020	0.220	950.0	840.0		
Interior slab	Finishing layer	0.020	0.220	950.0	840.0	2.841	494.12
	Structural layer	0.200	1.730	2245.6	836.8		
	Regulation layer	0.010	0.220	950.0	840.0		
	Finishing layer	0.020	0.200	825.0	2385.0		

k – thermal conductivity, ρ – density, c_p – specific heat, U – thermal transmittance.

Table 9
Thermophysical properties of the building elements for the lightweight construction that are fixed. Based on Ref. [27].

Element	Layer	Thick. (m)	k (W·m^{-1}·K^{-1})	ρ (kg·m^{-3})	c_p (J·kg^{-1}·K^{-1})	U (W·m^{-2}·K^{-1})	Mass (kg·m^{-2})
Interior wall	Finishing layer	0.013	0.250	900.0	1000.0	0.763	60.55
	Regulation layer	0.012	0.130	650.0	1700.0		
	Foam layer	0.002	0.050	30.0	2400.0		
	Structural/core layer	0.100	0.110	214.3	656.4		
	Foam layer	0.002	0.050	30.0	2400.0		
	Regulation layer	0.012	0.130	650.0	1700.0		
	Finishing layer	0.013	0.250	900.0	1000.0		
Interior slab	Finishing layer	0.013	0.250	900.0	1000.0	0.425	64.36
	OSB layer	0.012	0.130	650.0	1700.0		
	Foam layer	0.002	0.050	30.0	2400.0		
	Structural/core layer	0.300	0.160	55.0	561.6		
	Foam layer	0.002	0.050	30.0	2400.0		
	OSB layer	0.025	0.130	650.0	1700.0		
	Finishing layer	0.010	0.170	1200.0	1400.0		

k – thermal conductivity, ρ – density, c_p – specific heat, U – thermal transmittance.

values in heavyweight and lightweight construction were determined. This calculation allows us to determine how thermal mass influences the correlation between geometry and energy consumed. The geometry indexes are grouped into two types: compactness-related and glazing-related indexes.

The compactness-related indexes are the Shape Factor—*Cf*; Eq. (1), where S is the total external surface of the building in contact with the outdoor air (m^2) and V the building volume in cubic meters—and the Relative Compactness—*RC;* Eq. (2), where S_{rv} is the 5/6 of the surface area of a cube (m^2) with the same volume as the building.

$$Cf = S/V \tag{1}$$

$$RC = S_{rv}/S \tag{2}$$

The glazing-related indexes are the Window-to-Surface Ratio—*WSR*; Eq. (3), where S_g is the total glazing surface area (m^2), and S is the total external surface area of the building (m^2)—, the Window-to-Wall Ratio—*WWR*; Eq. (4), where S_w is the external wall surface area of the building (m^2)—, and the Window-to-Floor Ratio—*WFR;* Eq. (5), where S_f is the building floor surface area (m^2).

$$WSR = S_g/S \tag{3}$$

$$WWR = S_g/S_w \tag{4}$$

$$WFR = S_g/S_f \tag{5}$$

3. Results

For ease of comparison, the 21 locations were grouped according to the trend of the ideal thermal transmittance values in Iran, as depicted in Fig. 4 and according to findings from Ref. [49]: Group 1 – locations where buildings will require higher U-values in the future (marked as blue squares), Group 2 – lower or equal values in the future (yellow triangles), and Group 3 – where values should be the lowest possible for the present day and the future (red circles). For each group, key weather variables influencing building energy performance in different timeframes are presented. Then, the differences between heavyweight and lightweight constructions for total energy intensity, cooling, and heating energy consumption across various timeframes are analyzed. Following this, the performance across the range of U-values and how these performances evolved over time are analyzed. Subsequently, the relationship between thermal mass and building geometry is discussed for each respective timeframe.

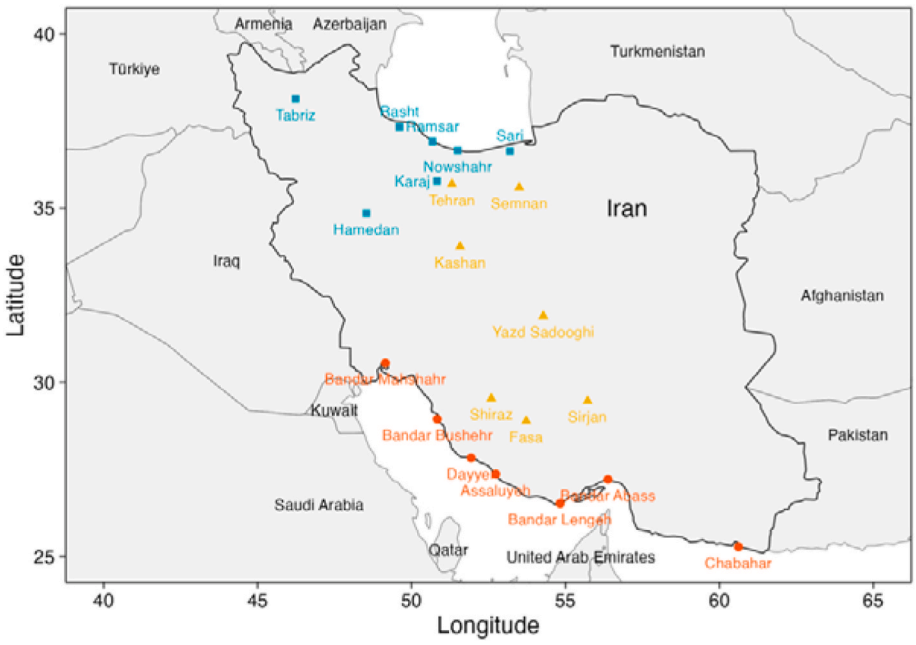

Fig. 4. Locations grouped according to Ref. [49]. Blue squares depict Group 1, yellow triangles Group 2, and red circles Group 3. (For interpretation of the references to color in this figure legend, the reader is referred to the Web version of this article.)

3.1. Group 1 – northern cities

The results from generating future weather show a rise in terms of daily average temperature, both daily minimum and maximum average temperatures, with a more pronounced effect observed in highland cities (Tabriz, Karaj, and Hamedan) compared to coastal areas (Rasht, Ramsar, Nowshahr, and Sari). Hamedan demonstrates the most substantial change, with a temperature increase of 4.6 °C in 2050 and 7.9 °C in 2080. Relatively to global horizontal radiation, it shows a slight decrease across the timeframes. The differences range from −2.1 $W{\cdot}h{\cdot}m^{-2}$ to −4.2 $W{\cdot}h{\cdot}m^{-2}$ in 2050 and from −1 $W{\cdot}h{\cdot}m^{-2}$ to −3.4 $W{\cdot}h{\cdot}m^{-2}$ in 2080.

Relative to the buildings' energy performance, the first column in Fig. 5 illustrates a percentage of the overall difference in yearly energy intensity between heavyweight and lightweight constructions. For all cities in Group 1, situated in Iran's northern and northwestern regions, the total energy difference consistently exhibits negative values across all three timeframes—differences ranging from −2 % to −10 % in the present day and 2050 and from −2 % to −8 % in 2080. Heavyweight construction presents lower energy intensity compared to lightweight construction for the present-day (green lines), 2050 (orange), and 2080 (red) timeframes. The differences in total energy intensity (heating plus cooling) vary between -0.68 ± 0.05 $kW{\cdot}h{\cdot}m^{-2}$ and -1.58 ± 0.04 $kW{\cdot}h{\cdot}m^{-2}$ in the present day, between -0.67 ± 0.05 $kW{\cdot}h{\cdot}m^{-2}$ and -1.51 ± 0.05 $kW{\cdot}h{\cdot}m^{-2}$ in 2050, and between -0.53 ± 0.06 $kW{\cdot}h{\cdot}m^{-2}$ and -1.48 ± 0.05 $kW{\cdot}h{\cdot}m^{-2}$ in 2080.

Assessing the outcomes across various *U*-values, it becomes evident that for low *U*-values, heavy thermal mass exhibits lower energy intensity (indicating higher energy efficiency), except for instances of very low *U*-values. However, as the *U*-values of the building envelope increase, the advantage of employing heavy thermal mass over lightweight structures diminishes.

Comparing the present-day to 2050 and 2080 timeframes in the cold cities of Tabriz, Karaj, and Hamedan, we note that buildings with higher thermal mass demonstrate improved energy performance in future timeframes (up to -0.48 $kW{\cdot}h{\cdot}m^{-2}$ and -0.83 $kW{\cdot}h{\cdot}m^{-2}$ compared to 2050 and 2080, respectively) except for very low *U*-values that show thermal mass increasing energy consumption (up to $+0.46$ $kW{\cdot}h{\cdot}m^{-2}$ in 2050 and $+0.52$ $kW{\cdot}h{\cdot}m^{-2}$ in 2080). In the coastal cities of Rasht, Ramsar, Nowshahr, and Sari, buildings with higher thermal mass exhibit lower energy intensity in the present-day climate than in the future around the whole range but are particularly advantageous for low *U*-values. For instance, the reduction may reach up to -0.50 $kW{\cdot}h{\cdot}m^{-2}$ in 2050 (34 % less than present-day climate construction differences) and -0.73 $kW{\cdot}h{\cdot}m^{-2}$ in 2080 (52 %). This implies that thermal mass becomes less energy-efficient in the warmer future projected for these coastal cities.

In all cases, the evolution of the total energy difference (diminishing advantage of employing heavyweight construction over lightweight for higher *U*-values) tends to follow the cooling difference evolution (second column in Fig. 5), which generally displays similar values for all timeframes. The difference in total energy between timeframes is mainly the result of the heating differences, as seen in the third column. Thus, for buildings located in this group, the impact of different thermal mass will mainly be on heating demand in the future.

Regarding the Coefficient of Determination (R^2) for the five geometry indexes, for the first group of cities, the first column of Fig. 6 shows that buildings with heavyweight construction materials have a stronger correlation between geometry indexes like Shape Factor (Cf) and relative compactness (*RC*) with energy consumption compared to lightweight structures during the current period. In simpler terms, changes in Cf and *RC* are more likely to impact the energy consumption of buildings with heavyweight construction than buildings with lightweight structures.

In contrast, for the same present-day timeframe, the correlation between glazing-related indexes (such as *WSR*, *WWR*, and *WFR*) and the energy consumption is weaker for heavyweight construction than for lightweight, meaning that windows play a more important role in the energy consumption of building with lightweight constructions than building with heavyweight construction. Noteworthy, for buildings with very low *U*-values, there is no difference between construction types; in other words, they have the same correlations with those factors.

Looking into the future, within the timeframes of 2050 and 2080, denoted by the second and third columns in Fig. 6, the color scheme, which represents the relevance of construction types with these factors and energy consumption, gradually fades. This indicates that the

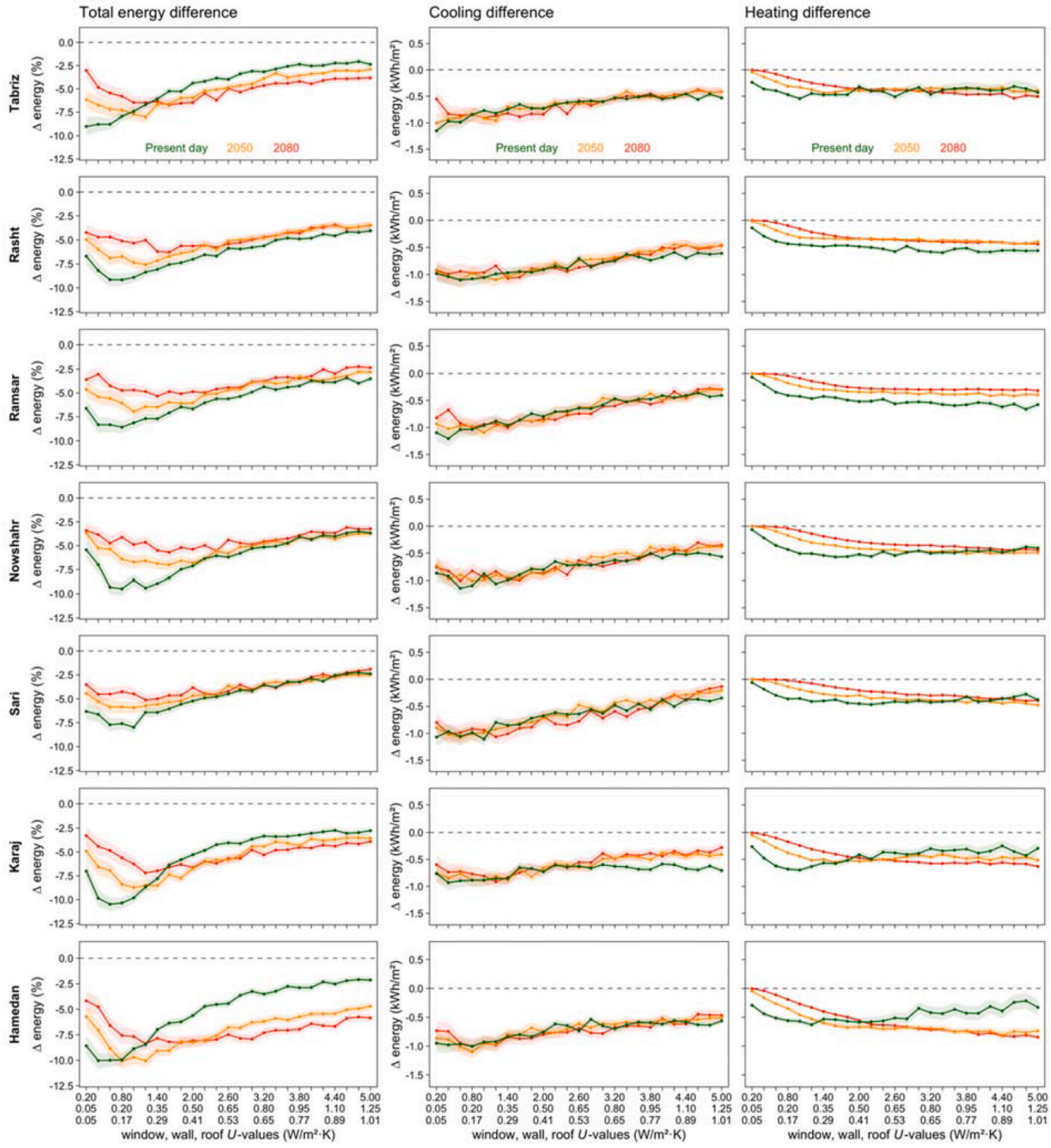

Fig. 5. Group 1 – Comparison of the differences in yearly energy intensity (kWh·m^{-2} of air-conditioned rooms) between heavyweight and lightweight constructions for the present-day (green lines), 2050 (orange), and 2080 (red) timeframes. Graphs in the first column depict the percentage difference in total energy consumed. Graphs in the second and third columns illustrate the absolute differences in cooling and heating energy consumed. Shadowed areas represent a 95 % confidence interval. Negative values mean heavyweight construction consumes less energy. (For interpretation of the references to color in this figure legend, the reader is referred to the Web version of this article.)

significance of construction type is diminishing over time. In other words, the thermal mass impact becomes less relevant regarding these geometry indexes as the climate continues to warm up.

3.2. Group 2 – central inland cities

In Group 2, the results of future weather generation show that the maximum average temperature will increase by 3.7 °C for 2050 and 7 °C for 2080, falling between the differences for highland and coastal cities

Fig. 6. Group 1 – Differences in Coefficient of Determination (R^2) values between thermal masses for each timeframe. Red cells depict heavyweight construction having a lower correlation between the index and energy consumption than lightweight construction. Green cells depict the opposite. (For interpretation of the references to color in this figure legend, the reader is referred to the Web version of this article.)

in Group 1, and daily minimum and maximum average temperatures also exhibit an upward trend. A slight decrease in global horizontal radiation for all cities in this group is expected, ranging from -3 W·h·m^{-2} in 2050 to -1 W·h·m^{-2} in 2080.

In Fig. 7, buildings constructed with heavy materials exhibit lower energy intensity than lightweight construction—differences ranging from -3 % to -8 % in the present day, from -2 % to -6 % in 2050, and from -2 % to -5 % in 2080. The differences vary between -0.79 ± 0.10 kW·h·m^{-2} and -1.56 ± 0.06 kW·h·m^{-2} in the present day, between -0.57 ± 0.10 kW·h·m^{-2} and -1.46 ± 0.07 kW·h·m^{-2} in 2050, and between -0.46 ± 0.10 kW·h·m^{-2} and -1.22 ± 0.07 kW·h·m^{-2} in 2080.

When we compare different timeframes for higher *U*-values, the energy intensity differences remain somewhat lower in the present-day or stay similar across all periods, except for the city of Fasa. However, the highest contrast between timeframes is noticeable at lower *U*-values, where heavy structures perform notably better in today's climate than in the future. For example, this reduction may reach up to -0.60 kW·h·m^{-2} in 2050 (44 % less than present-day climate construction differences) and -0.93 kW·h·m^{-2} in 2080 (63 %). To put it plainly, the reduced energy intensity observed across all *U*-value ranges for the present day suggests that thermal mass currently performs better than it will in the warmer future. As in Group 1, cities in this group also show that adequate *U*-values will enhance the energy benefits of a higher thermal mass.

As in Group 1, the evolution of the total energy difference also tends to follow the cooling difference evolution (second column), with the difference in total energy between timeframes mainly the result of the heating differences (third column). The third column now displays higher and more constant differences in heating between timelines than in Group 1.

Regarding the geometry indexes (Fig. 8), we observe a trend similar to that of the first group. Heavy construction exhibits a more pronounced correlation with compactness-related indexes and energy consumption. At the same time, a weaker link is observed between glazing-related indexes and energy consumption when compared with light construction. Similar to Group 1, the importance of the building construction material, whether heavy or light, decreases over time, illustrated by the fading colors as we move from the present to the future.

3.3. Group 3 – southern coastal cities

The generated future weather shows a consistent increase in the average dry bulb temperature for all locations in this group, similar to the patterns observed in cities of Groups 1 and 2. However, compared to other groups, they show lower temperature differences across timeframes. The maximum average dry bulb temperature increase is observed at 2.8 °C for 2050 and 5.2 °C for 2080. Differences between the daily minimum and maximum average temperatures for cities in this group are lower than in other cities but still show an upward trend over the timeframes. Global horizontal radiation exhibits a slight decrease for all cities, ranging from -4.1 W·h·m^{-2} in 2050 to -3.4 W·h·m^{-2} in 2080.

Group 3 presents cities with high demand for cooling (Fig. 9) and shows negative energy intensity values across nearly all *U*-value ranges. Although with diminished benefits than in the previous two groups, heavyweight construction still outperforms lightweight construction in almost the whole range of thermal transmittances—differences varying from -4 % to none in present-day and 2050 and from -3 % and $+1$ % in 2080. The differences vary between $+0.18 \pm 0.10$ kW·h·m^{-2} and -1.28 ± 0.11 kW·h·m^{-2} in present day, between $+0.06 \pm 0.11$ kW·h·m^{-2} and -1.32 ± 0.11 kW·h·m^{-2} in 2050, and between $+0.39 \pm 0.11$ kW·h·m^{-2} and -1.33 ± 0.11 kW·h·m^{-2} in 2080. However, it is important to point out that this difference diminishes to zero in cases of very high *U*-values. This result indicates that, in buildings with inadequate insulation, the type of construction (heavyweight or lightweight) does not significantly impact performance in this exceedingly warm region. When we evaluate thermal performance across various timeframes, we observe that the differences remain consistent across the entire *U*-value spectrum for all cities of this group, showing buildings in the present day to have lower consumption, up to -0.54 kW·h·m^{-2} (42 % less than present-day climate construction differences) and -0.70 kW·h·m^{-2} (100 %), compared to 2050 and 2080, respectively.

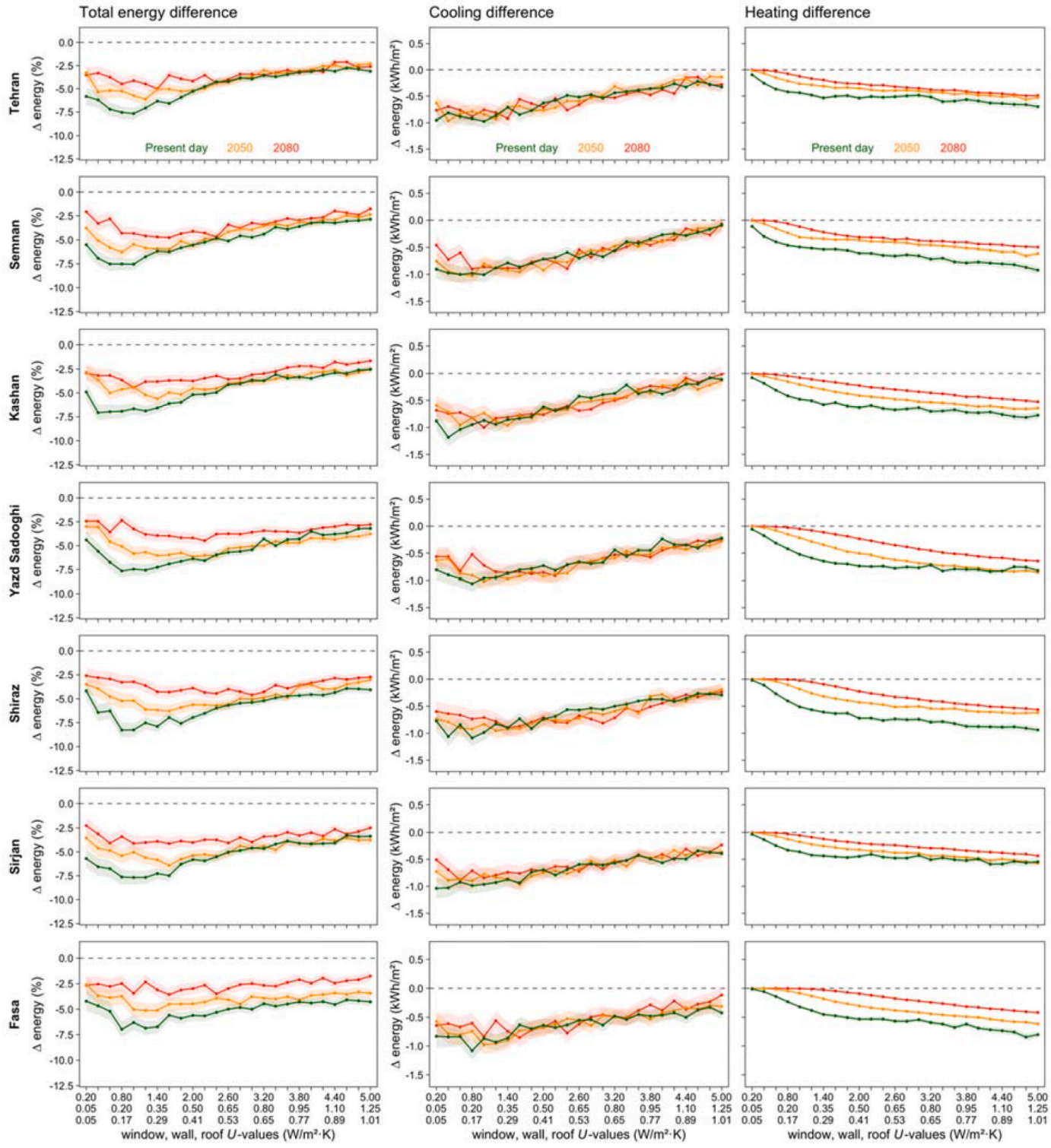

Fig. 7. Group 2 – Comparison of the differences in yearly energy intensity (kWh·m^{-2} of air-conditioned rooms) between heavyweight and lightweight constructions for the present-day (green lines), 2050 (orange), and 2080 (red) timeframes. Graphs in the first column depict the percentage difference in total energy consumed. Graphs in the second and third columns illustrate the absolute differences in cooling and heating energy consumed. Shadowed areas represent a 95 % confidence interval. Negative values mean heavyweight construction consumes less energy. (For interpretation of the references to color in this figure legend, the reader is referred to the Web version of this article.)

The evolution of the total energy difference closely follows the cooling difference evolution, as seen in the second column in Fig. 9. The heating differences between construction types are very small or even inexistent (third column) due to the very low or null heating requirements in the locations of this group.

In Fig. 10, concerning the geometry indexes, it is observed that the color scheme remains consistently pale throughout all periods, even for the current time. This consistent trend reveals that in these warm climate cities, the classification of construction types, be it heavy or light, carries minimal significance. In simpler terms, there is no notable

Fig. 8. Group 2 – Differences in Coefficient of Determination (R^2) values between thermal masses for each timeframe. Red cells depict heavyweight construction having a lower correlation between the index and energy consumption than lightweight construction. Green cells depict the opposite. (For interpretation of the references to color in this figure legend, the reader is referred to the Web version of this article.)

difference in the correlation between geometry indexes and energy consumption for buildings with high and low thermal mass. Therefore, in warmer climates, using thermal mass does not provide a significant advantage in affecting energy consumption over lightweight constructions.

4. Discussion

Comparing Groups 1, 2, and 3 provides valuable insights. Firstly, we observe that the differences in energy intensity between heavy and light thermal mass are more pronounced in cities within Groups 1 and 2 than in Group 3. This finding underscores the idea that in cities with higher heating demand (Groups 1 and 2), heavy construction can prove to be more effective than lightweight construction, resulting in greater energy savings, as solar heat is captured during the day and released at nighttime when the building is permanently occupied. This confirms the findings of previous works addressing the same climate (*e.g.*, Shiraz [36] and Tehran [37]) or similar (*e.g.*, Cairo [8], Riyadh [9], Al-Ain [19], and Beer Sheva [20]), which point to the reduction and stabilization of indoor temperatures by employing heavy construction, thus avoiding overheating and decreasing thermal energy demands.

Secondly, across all cities, it becomes apparent that construction with lower thermal transmittance (although not at extremely low levels) tends to favor heavy thermal mass over lightweight alternatives. Nevertheless, this effectiveness diminishes as *U*-values increase. This finding echoes a common theme in existing literature, including other studies in Iran [36,37], suggesting that combining effective insulation with heavy thermal mass can lead to more efficient outcomes.

Considering cooling demand (the second column in Figs. 5, 7 and 9), it is consistently observed that heavyweight construction always requires less cooling energy (ranging from -1.5 kWh·m^{-2} to none) for all cities and across all timeframes, reflecting other the findings in the literature for the same climate type. The overlap of the three timeframe lines underscores the similar thermal mass performance concerning cooling demand over time. Considering the range of *U*-values, heavyweight construction performs better at lower *U*-values for all cities. Nonetheless, in buildings located in warm climates (Group 3) with inadequate insulation (very high *U*-values), it is noticeable that heavy construction consumes energy nearly equal to lightweight construction or even slightly more across all timeframes.

However, an inverse trend is observed for heating demand (the third column in Figs. 5, 7 and 9). There is virtually no difference between heavy and light constructions at very low *U*-values. As we progress towards higher thermal transmittances, buildings with heavy construction consume less heating energy across all cities in Groups 1 and 2 for all timeframes. This result highlights the advantage of using thermal mass for buildings with inadequate insulation in climates where heating demand prevails.

Furthermore, when we consider different timeframes, it is obvious that as the climate gradually warms, the effectiveness of thermal mass compared to lightweight construction declines (with current-day values consistently lower than those of 2050, the latter lower than those of 2080). This trend holds for Group 3, where heating demand is minimal. In cases where heating demand is present, the pattern aligns with that observed in Groups 1 and 2. The only comparable results in the literature refer to a study in the arid climate of Al-Ain (UAE) [19], which points to a significant reduction of energy use for heating and cooling in the present and future by employing higher thermal mass. However, the comparison cannot be made lightly since (i) the future scenarios considered differ from the one in the present work (Table 2) and (ii) the thermal transmittances for walls (2.32 W·m^{-2}·K) and windows (6.3 W·m^{-2}·K) are far greater than the maximum values admitted in the present study. Nevertheless, the results confirm that heavier buildings present an advantage in energy performance in the present day, while in the future, the trend is highly dependent on the scenario but still clearly advantageous for high thermal mass, with the authors stating that the amount of energy saved due to a higher thermal mass is increased as the ambient air temperature gets warmer, leading to greater energy savings. Our findings contradict such conclusions, as shown by our results for future climates (*i.e.*, less effectiveness of thermal mass), especially for high *U*-values, as in Ref. [19]. In addition, our work presents a far more in-depth analysis, contributing more thorough and novel results, even

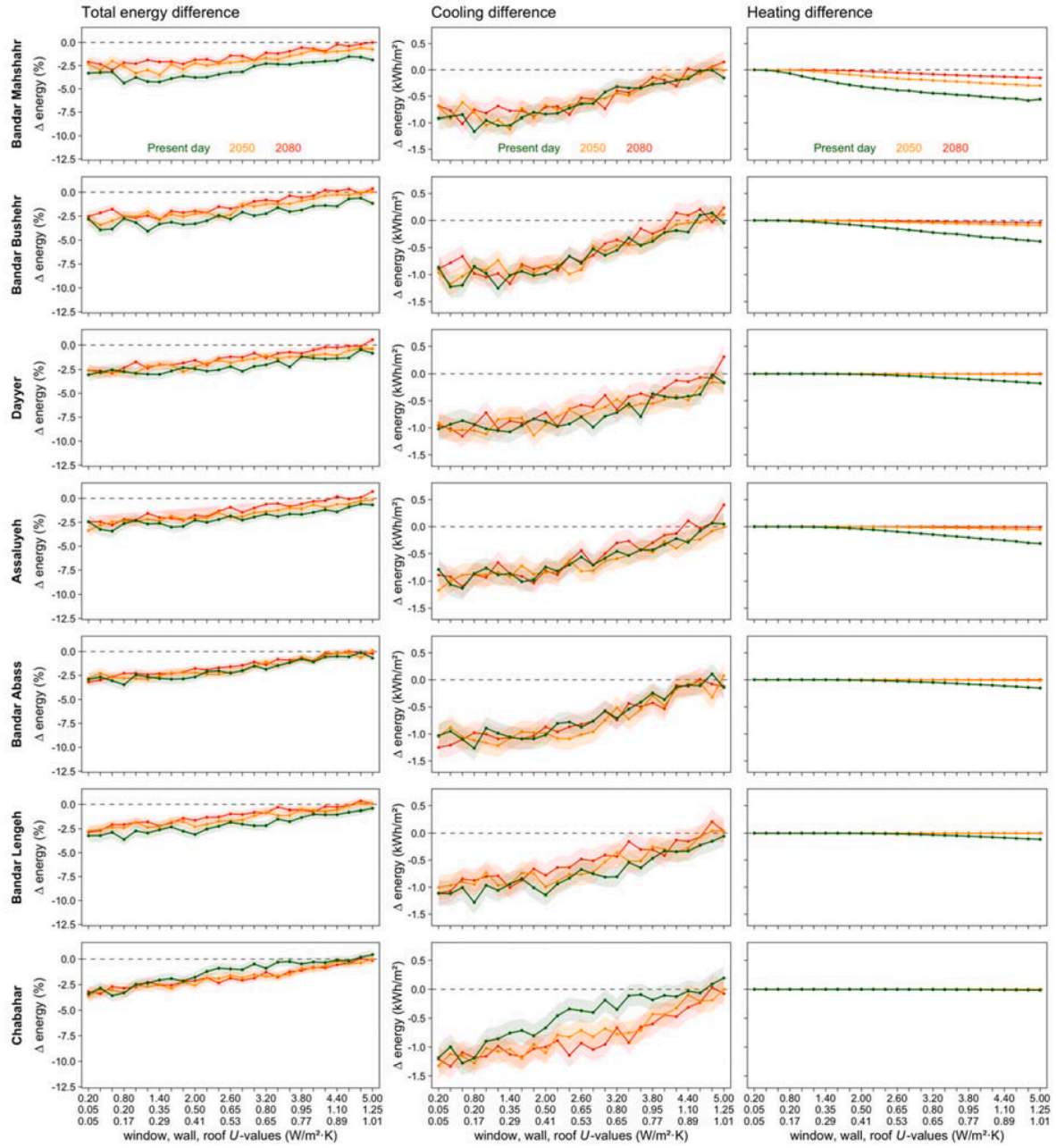

Fig. 9. Group 3 – Comparison of the differences in yearly energy intensity (kWh·m^{-2} of air-conditioned rooms) between heavyweight and lightweight constructions for the present-day (green lines), 2050 (orange), and 2080 (red) timeframes. Graphs in the first column depict the percentage difference in total energy consumed. Graphs in the second and third columns illustrate the absolute differences in cooling and heating energy consumed. Shadowed areas represent a 95 % confidence interval. Negative values mean heavyweight construction consumes less energy. (For interpretation of the references to color in this figure legend, the reader is referred to the Web version of this article.)

when compared with the few other studies that also address the impact of climate change on energy performance (Table 2).

Several noteworthy observations regarding the buildings' geometry emerge when comparing Groups 1, 2, and 3. Firstly, as we move from colder cities in the northern regions and center (Groups 1 and 2) to the significantly warmer cities in southern Iran (Group 3), a reduction in the difference in the correlation between geometric indicators and energy consumption for buildings constructed with heavyweight and lightweight constructions becomes evident. This trend is represented by the fading colors during the transition from northern to southern cities within the same timeframe, aligning with our previous observations across all cities moving from the present to the future. In summary, heavyweight constructions do not confer any advantage over their lightweight counterparts regarding the building's geometry when considering the shift toward warmer climates or the expectation of a warmer future. This is also true for very low *U*-values in all locations.

4.1. Limitations and future work

This study has some limitations that, if overcome, may provide a different understanding of the results. The functional program we used was a generic two-story single-family house whose representativeness is unknown due to the lack of statistical information about the current Iranian built environment [70]. In addition, no study refers to building archetypes in this region based on statistical data that could be used as a reference to adjust the generated buildings.

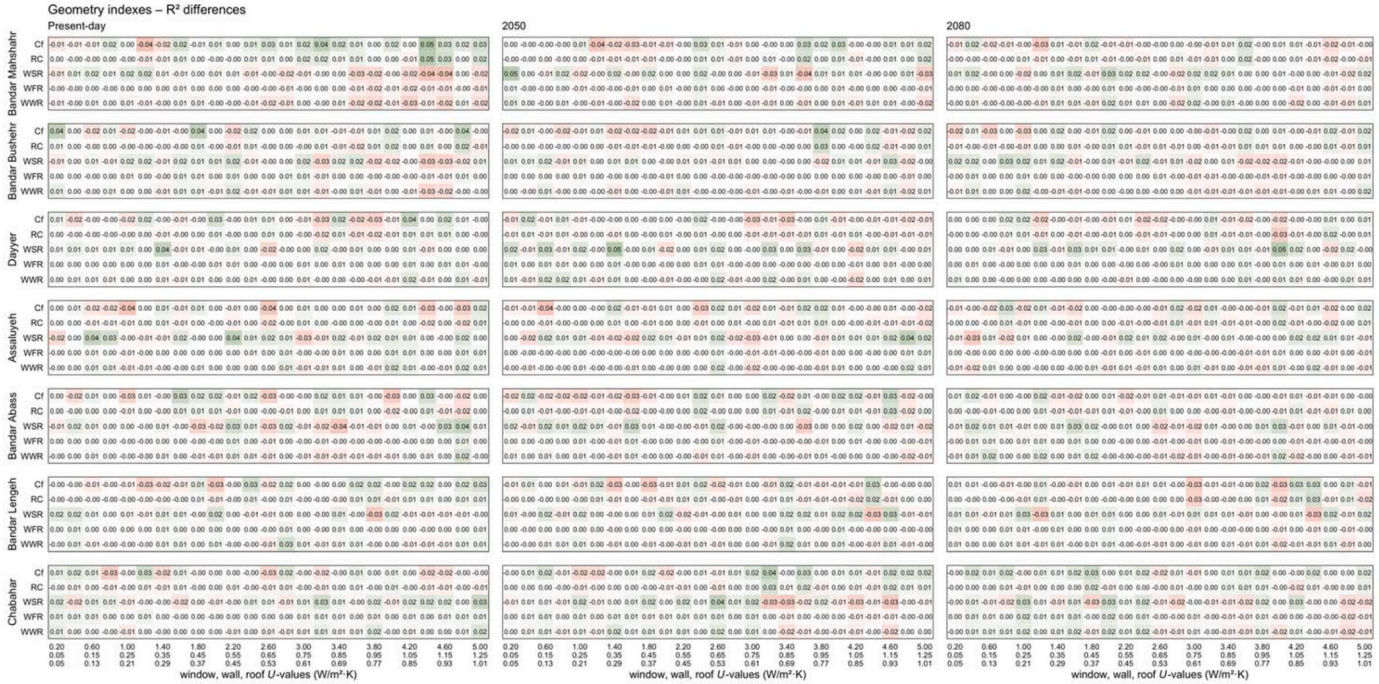

Fig. 10. Group 3 – Differences in Coefficient of Determination (R^2) values between thermal masses for each timeframe. Red cells depict heavyweight construction having a lower correlation between the index and energy consumption than lightweight construction. Green cells depict the opposite. (For interpretation of the references to color in this figure legend, the reader is referred to the Web version of this article.)

To have a basis for comparison among different cities, thermal mass, thermal transmittances, and climate scenarios, we defined constant and low-rate ventilation values similar to those found in high-performance buildings. However, this simplification ignores the fact that ventilation may play a role in minimizing overheating [71]. As ventilation works when outdoor conditions allow the exchange of indoor hot air with outdoor colder air, cities in Group 1 and several from Group 2 would benefit from it, particularly during nighttime. However, we predict its use will reduce as global warming settles in, and fewer hours of colder outdoor air will be available in the future. In a few cities in Group 2 and all cities in Group 3, such a strategy does not work, as the outdoor air is constantly above the cooling setpoint in the present-day climate. It should also be noted that using dynamic ventilation strategies would diminish the differences between construction types, and ultimately, lightweight construction could prove to be more energy-efficient in colder regions.

Similar reasoning was used regarding windows' solar gains. Again, to make a fair comparison, we decided to have fixed SHGC and VT values, although these values tend to decrease as the window's thermal transmittance also decreases. These lower values would lead to lower cooling needs and more heating needs, particularly in the Northern cities in Iran, or lower cooling needs in the Southern cities. However, because these values are the same for both construction types and we only determine the differences between them, we foresee that varying SHGC and VT values would diminish the benefit of thermal mass even further, especially in the low range of thermal transmittances.

Another aspect related to solar gains is windows' shades. The study assumes shades are active during nighttime to prevent heat losses and provide privacy and safety. Therefore, buildings capture solar radiation during the daytime, when vacated, to raise indoor temperatures for nighttime occupancy. This strategy works well in central and northern Iran's colder cities but not in southern cities. Therefore, this strategy neglects that shades could be active during the daytime to reduce the cooling needs, particularly in some cities in Group 2 and all Southern cities in Group 3. However, because shades are activated in both construction types in the same way and we are calculating the differences for comparison, we foresee no great differences in the results or, eventually, a benefit for lightweight constructions.

This study exclusively examines the buildings' operational energy consumption, overlooking the embodied energy of materials, which may markedly affect the overall environmental footprint of buildings. Therefore, we foresee lightweight construction having higher energy savings overall if we include the embodied energy of materials, particularly in the future. Consequently, further research should encompass a more comprehensive analysis that considers energy utilization during a building's lifecycle and accounts for the energy embedded in construction materials. This approach would provide a more global view of the environmental consequences related to the selection of different construction materials. In addition, future research should focus on overcoming the stated limitations to have a deeper understanding of the role of thermal mass, such as determining statistical data representative of the built environment in the region, studying the effects of solar gains through glazed areas with varying optic properties, and analyzing different ventilation strategies.

4.2. *Recommendations*

This study uncovers important insights into the relationship between construction materials and building energy efficiency in Iran. The selection of heavy construction materials in the colder regions of this country delivers observable energy savings. In contrast, in warmer climates, the emphasis should shift towards energy-efficient design principles to reduce energy consumption effectively. It is imperative to understand that the long-term importance of material choice may diminish, particularly under warmer climatic conditions. Considering the study's results, some practical building strategies and recommendations based on this study can be summarized as follows.

Architects, practitioners, and technologists

- Prioritize heavyweight construction, such as concrete or masonry, particularly in cold regions and when using low *U*-values. However, they may consider lightweight construction for warmer coastal regions that allow for better ventilation and reduced cooling demands.
- Focus on optimizing the building envelope's *U*-value. This may result in highly insulated solutions and compact building designs in colder climates. In warmer climates, strategic use of shading devices and low *U*-value windows can minimize heat gain and cooling needs. Optimized *U*-values will also enhance the benefits of thermal mass.
- Consider the correlation between thermal mass and building geometry. For heavy construction, architects may emphasize compactness-related factors, such as optimizing shape factor and relative compactness, to maximize energy efficiency. In lightweight construction, strategies include selecting high-performance windows and glazing to improve overall building performance.
- Adopt other climate-adaptive design strategies because thermal mass will lose its importance. For example, architects may explore flexible design features, such as operable shading systems, natural ventilation solutions, and renewable energy integration, to ensure buildings remain energy efficient.

Policymakers and municipal authorities

- Integrate the study's findings into building codes. By introducing new provisions or guidelines, they can promote the strategic use of thermal mass, considering specific factors and the effect of climate change. In regions like Iran, where existing codes may lack recommendations for thermal mass utilization, incorporating insights from this study can substantially reduce energy consumption. For instance, while the current building code of Iran focuses on low *U*-values for different climate regions, updating regulations to include considerations for thermal mass can lead to more regional construction practices (with low *U*-values, in colder regions, heavyweight construction may be preferable, while lighter construction options could be recommended for warmer coastal areas). Also, based on the study's findings, there should be a heightened focus on selecting high-performance windows and transparent elements in warmer regions and compactness-related factors for colder climates in the building code.
- Offer incentives or subsidies to developers and builders who implement the energy-efficient building strategies outlined in the study. Encourage the use of appropriate materials, design strategies, and technologies that align with sustainability goals and contribute to reducing environmental impact.

The findings of this study not only provide valuable insights but also open new research paths. Investigating the embodied energy within construction materials is paramount to comprehensively assessing diverse building materials' environmental impact. Furthermore, future studies could comprehensively evaluate the cost implications of selecting heavy or lightweight construction materials in different climatic regions. This evaluation entails analyzing how construction material choices influence initial and long-term operational costs, providing a more holistic view of the economic dimensions of these decisions. These potential research areas are intriguing and hold significant promise for further exploration.

5. Conclusions

In this comprehensive study, encompassing diverse climatic conditions in Iran, we addressed three key questions related to the energy impacts of climate change on heavyweight and lightweight constructions. Regarding the main question, "Will thermal mass remain effective in the future?" we conclude that it will significantly lose its effectiveness as a passive design strategy. However, this is not completely true in a few cities in Northern Iran, where thermal transmittances are between mid-to very high-range values.

This finding provides insight into the second question: "How do variations in *U*-values and climate impact the role of thermal mass in buildings?" In fact, heavyweight buildings in three cities with mid to high *U*-values will have greater energy performance than those with lightweight construction in the future climate, and the opposite is found in the low *U*-values. In the remaining cities, except those in Southern Iran, heavyweight buildings with low *U*-values tend to lose their energy-saving edge in the future. In contrast, climate change will not be so impactful in the remaining range. Also, independently of the climate scenario, mid-to very high-range *U*-values tend to minimize the effect of thermal mass.

Regarding the last question, "Will thermal mass affect the building geometry options?" we conclude that heavyweight buildings exhibit a stronger correlation between energy consumption and compactness-related indexes and lightweight construction with glazing-related indexes in present-day climate. However, as the climate gets warmer or we move towards warmer regions in Iran, these correlations attenuate or become inexistent. Lastly, as climate change settles in and thermal mass loses its benefits, building professionals will lose one of their most important design strategies but will gain a wider range of construction materials and will become freer to choose alternative designs.

Our findings are summarized as follows.

- Over time, the importance of thermal mass diminishes in all locations, particularly in warmer regions and the future, eliminating its energy-saving edge.
- In warmer climates, thermal mass has minimal impact on energy consumption.
- In Tabriz, Karaj, and Hamedan (Northwest Iran), heavyweight construction will present energy benefits from rising temperatures for mid to very-high thermal transmittances. However, buildings with low thermal transmittances will have the opposite effect from thermal mass.
- Correlation analysis reveals that heavyweight construction exhibits stronger links with energy consumption through compactness-related indexes, while lightweight construction is more associated with glazing-related indexes.
- Adequate envelope *U*-values will enhance the energy benefits of having higher thermal mass, and building practitioners should consider them both when deciding on a construction solution, particularly in central and northern cities in Iran.
- In general, heavy thermal mass loses impact in a warmer future or region, underlining the shifting dynamics of building energy efficiency.

CRediT authorship contribution statement

Eugénio Rodrigues: Writing – review & editing, Writing – original draft, Visualization, Supervision, Software, Project administration, Methodology, Investigation, Funding acquisition, Formal analysis, Data curation, Conceptualization. **Nazanin Azimi Fereidani:** Writing – review & editing, Writing – original draft, Investigation, Formal analysis, Conceptualization. **Marco S. Fernandes:** Writing – review & editing, Software, Investigation, Formal analysis, Conceptualization. **Adélio R. Gaspar:** Writing – review & editing, Supervision, Resources, Conceptualization.

Declaration of competing interest

The authors declare that they have no known competing financial interests or personal relationships that could have appeared to influence the work reported in this paper.

Data availability

Data will be made available on request.

Acknowledgments

The presented work is framed under the *Energy for Sustainability Initiative* of the University of Coimbra (UC).

We acknowledge the World Climate Research Programme, which, through its Working Group on Coupled Modelling, coordinated and promoted CMIP6. In addition, we thank the climate modeling groups for producing and making their model output available, the Earth System Grid Federation (ESGF) for archiving and providing access to the data, and the multiple funding agencies that support CMIP6 and ESGF.

The Portuguese Foundation for Science and Technology (FCT) supported this work [PTDC/EME-REN/3460/2021 doi:10.54499/PTDC/EME-REN/3460/2021 and UIDB/50022/2020 doi:10.54499/UIDB/50022/2020]. In addition, FCT supports Eugénio Rodrigues [2021.00230.CEECIND doi:10.54499/2021.00230.CEECIND/CP1681/CT0001] and Marco S. Fernandes [2021.02975.CEECIND doi:10.54499/2021.02975.CEECIND/CP1681/CT0002] through researcher contracts, and Nazanin Azimi Fereidani through a Ph.D. fellowship [SFRH/BD/151355/2021].

The authors are thankful to Prof. José Joaquim Costa for his comments and suggestions.

References

[1] T. Hong, J. Malik, A. Krelling, W. O'Brien, K. Sun, R. Lamberts, M. Wei, Ten questions concerning thermal resilience of buildings and occupants for climate adaptation, Build. Environ. 244 (2023) 110806, https://doi.org/10.1016/j.buildenv.2023.110806.

[2] J.N. Hacker, T.P. De Saulles, A.J. Minson, M.J. Holmes, Embodied and operational carbon dioxide emissions from housing: a case study on the effects of thermal mass and climate change, Energy Build. 40 (2008) 375–384, https://doi.org/10.1016/j.enbuild.2007.03.005.

[3] K. Gregory, B. Moghtaderi, H. Sugo, A. Page, Effect of thermal mass on the thermal performance of various Australian residential constructions systems, Energy Build. 40 (2008) 459–465, https://doi.org/10.1016/j.enbuild.2007.04.001.

[4] T. Kuczyński, A. Staszczuk, Experimental study of the influence of thermal mass on thermal comfort and cooling energy demand in residential buildings, Energy 195 (2020) 116984, https://doi.org/10.1016/j.energy.2020.116984.

[5] T. Kuczyński, A. Staszczuk, P. Ziembicki, A. Paluszak, The effect of the thermal mass of the building envelope on summer overheating of dwellings in a temperate climate, Energies 14 (2021) 4117, https://doi.org/10.3390/en14144117.

[6] J. Deng, R. Yao, W. Yu, Q. Zhang, B. Li, Effectiveness of the thermal mass of external walls on residential buildings for part-time part-space heating and cooling using the state-space method, Energy Build. 190 (2019) 155–171, https://doi.org/10.1016/j.enbuild.2019.02.029.

[7] S. Kumar, M.K. Singh, A. Mathur, S. Mathur, J. Mathur, Thermal performance and comfort potential estimation in low-rise high thermal mass naturally ventilated office buildings in India: an experimental study, J. Build. Eng. 20 (2018) 569–584, https://doi.org/10.1016/j.jobe.2018.09.003.

[8] W.A.Y. Mousa, W. Lang, W.A. Yousef, Simulations and quantitative data analytic interpretations of indoor-outdoor temperatures in a high thermal mass structure, J. Build. Eng. 12 (2017) 68–76, https://doi.org/10.1016/j.jobe.2017.05.007.

[9] E. Alayed, D. Bensaid, R. O'Hegarty, O. Kinnane, Thermal mass impact on energy consumption for buildings in hot climates: a novel finite element modelling study comparing building constructions for arid climates in Saudi Arabia, Energy Build. 271 (2022) 112324, https://doi.org/10.1016/j.enbuild.2022.112324.

[10] A.F. Krelling, R. Lamberts, J. Malik, T. Hong, A simulation framework for assessing thermally resilient buildings and communities, Build. Environ. 245 (2023) 110887, https://doi.org/10.1016/j.buildenv.2023.110887.

[11] A. Reilly, O. Kinnane, The impact of thermal mass on building energy consumption, Appl. Energy 198 (2017) 108–121, https://doi.org/10.1016/j.apenergy.2017.04.024.

[12] B. Hudobivnik, L. Pajek, R. Kunič, M. Košir, FEM thermal performance analysis of multi-layer external walls during typical summer conditions considering high intensity passive cooling, Appl. Energy 178 (2016) 363–375, https://doi.org/10.1016/j.apenergy.2016.06.036.

[13] T. Kuczyński, A. Staszczuk, M. Gortych, R. Stryjski, Effect of thermal mass, night ventilation and window shading on summer thermal comfort of buildings in a temperate climate, Build. Environ. 204 (2021) 108126, https://doi.org/10.1016/j.buildenv.2021.108126.

[14] H. Sun, J.K. Calautit, C. Jimenez-Bescos, Examining the regulating impact of thermal mass on overheating, and the role of night ventilation, within different climates and future scenarios across China, Clean. Eng. Technol. 9 (2022) 100534, https://doi.org/10.1016/j.clet.2022.100534.

[15] L. Pajek, M. Možina, P.D. Nadarajah, M.K. Singh, M. Košir, Future-proofing a naturally ventilated log house: a case study of adaptive thermal comfort under climate change impact, Energy Build. 307 (2024) 113951, https://doi.org/10.1016/j.enbuild.2024.113951.

[16] C. Jimenez-Bescos, An evaluation on the effect of night ventilation on thermal mass to reduce overheating in future climate scenarios, Energy Proc. 122 (2017) 1045–1050, https://doi.org/10.1016/j.egypro.2017.07.476.

[17] H. Wang, Q. Chen, A semi-empirical model for studying the impact of thermal mass and cost-return analysis on mixed-mode ventilation in office buildings, Energy Build. 67 (2013) 267–274, https://doi.org/10.1016/j.enbuild.2013.08.025.

[18] L. Zhu, R. Hurt, D. Correia, R. Boehm, Detailed energy saving performance analyses on thermal mass walls demonstrated in a zero energy house, Energy Build. 41 (2009) 303–310, https://doi.org/10.1016/j.enbuild.2008.10.003.

[19] H. Radhi, Evaluating the potential impact of global warming on the UAE residential buildings – a contribution to reduce the CO2 emissions, Build. Environ. 44 (2009) 2451–2462, https://doi.org/10.1016/j.buildenv.2009.04.006.

[20] E. Zilberberg, P. Trapper, I.A. Meir, S. Isaac, The impact of thermal mass and insulation of building structure on energy efficiency, Energy Build. 241 (2021) 110954, https://doi.org/10.1016/j.enbuild.2021.110954.

[21] I.J.A. Callejas, R.M. Apolonio, E.L.A. Da Guarda, L.C. Durante, K. de Andrade Carvalho Rosseti, F. Roseta, L.M. Do Amarante, Bermed earth-sheltered wall for low-income house: thermal and energy measure to face climate change in tropical region, Appl. Sci. 11 (2021) 420, https://doi.org/10.3390/app11010420.

[22] A. Dodoo, L. Gustavsson, R. Sathre, Effect of thermal mass on life cycle primary energy balances of a concrete- and a wood-frame building, Appl. Energy 92 (2012) 462–472, https://doi.org/10.1016/j.apenergy.2011.11.017.

[23] Y. Shang, F. Tariku, Hempcrete building performance in mild and cold climates: integrated analysis of carbon footprint, energy, and indoor thermal and moisture buffering, Build. Environ. 206 (2021) 108377, https://doi.org/10.1016/j.buildenv.2021.108377.

[24] N. Aste, A. Angelotti, M. Buzzetti, The influence of the external walls thermal inertia on the energy performance of well insulated buildings, Energy Build. 41 (2009) 1181–1187, https://doi.org/10.1016/j.enbuild.2009.06.005.

[25] N. Aste, F. Leonforte, M. Manfren, M. Mazzon, Thermal inertia and energy efficiency – parametric simulation assessment on a calibrated case study, Appl. Energy 145 (2015) 111–123, https://doi.org/10.1016/j.apenergy.2015.01.084.

[26] F. Stazi, E. Tomassoni, C. Bonfigli, C. Di Perna, Energy, comfort and environmental assessment of different building envelope techniques in a Mediterranean climate with a hot dry summer, Appl. Energy 134 (2014) 176–196, https://doi.org/10.1016/j.apenergy.2014.08.023.

[27] E. Rodrigues, M.S. Fernandes, A.R. Gaspar, Á. Gomes, J.J. Costa, Thermal transmittance effect on energy consumption of Mediterranean buildings with different thermal mass, Appl. Energy 252 (2019) 113437, https://doi.org/10.1016/j.apenergy.2019.113437.

[28] S. Verbeke, A. Audenaert, Thermal inertia in buildings: a review of impacts across climate and building use, Renew. Sustain. Energy Rev. 82 (2018) 2300–2318, https://doi.org/10.1016/j.rser.2017.08.083.

[29] R. Sharston, S. Murray, The combined effects of thermal mass and insulation on energy performance in concrete office buildings, Adv. Build. Energy Res. 14 (2020) 322–337, https://doi.org/10.1080/17512549.2018.1547220.

[30] R. Sharston, M.M. Ali, Parametric study of thermal mass property of concrete buildings in US climate zones, Archit. Sci. Rev. 56 (2013) 103–117, https://doi.org/10.1080/00038628.2012.729310.

[31] S.A. Al-Sanea, M.F. Zedan, Improving thermal performance of building walls by optimizing insulation layer distribution and thickness for same thermal mass, Appl. Energy 88 (2011) 3113–3124, https://doi.org/10.1016/j.apenergy.2011.02.036.

[32] S.A. Al-Sanea, M.F. Zedan, S.N. Al-Hussain, Effect of thermal mass on performance of insulated building walls and the concept of energy savings potential, Appl. Energy 89 (2012) 430–442, https://doi.org/10.1016/j.apenergy.2011.08.009.

[33] B. Salehpour, M. Ghobadi, H. Ge, T. Moore, Effects of thermal mass on transient thermal performance of concrete-based walls and energy consumption of an office building, J. Build. Phys. 47 (2023) 92–120, https://doi.org/10.1177/17442591231167609.

[34] M. Haj Hussein, S. Monna, A. Juaidi, A. Barlet, M. Baba, D. Bruneau, Effect of thermal mass of insulated and non-insulated walls on building thermal performance and potential energy saving, J. Phys. Conf. Ser. 2042 (2021) 012159, https://doi.org/10.1088/1742-6596/2042/1/012159.

[35] P.M. Congedo, C. Baglivo, G. Centonze, Walls comparative evaluation for the thermal performance improvement of low-rise residential buildings in warm Mediterranean climate, J. Build. Eng. 28 (2020) 101059, https://doi.org/10.1016/j.jobe.2019.101059.

[36] B. Rosti, A. Omidvar, N. Monghasemi, Optimum position and distribution of insulation layers for exterior walls of a building conditioned by earth-air heat exchanger, Appl. Therm. Eng. 163 (2019) 114362, https://doi.org/10.1016/j.applthermaleng.2019.114362.

[37] S. Memarian, B.M. Kari, S. Asadi, R. Fayaz, Building envelope thermal mass and its effect on spring and the Autumn seasonal transition period, J. Archit. Eng. 26 (2020) 1–13, https://doi.org/10.1061/(ASCE)AE.1943-5568.0000391.

[38] S. Flores-Larsen, C. Filippín, G. Barea, Impact of climate change on energy use and bioclimatic design of residential buildings in the 21st century in Argentina, Energy Build. 184 (2019) 216–229, https://doi.org/10.1016/j.enbuild.2018.12.015.

[39] M. Kottek, J. Grieser, C. Beck, B. Rudolf, F. Rubel, World Map of the Köppen-Geiger climate classification updated, Meteorol. Zeitschrift 15 (2006) 259–263, https://doi.org/10.1127/0941-2948/2006/0130.

[40] Original CMIP2 Announcement. https://pcmdi.llnl.gov/mips/cmip2/, 1997. (Accessed 12 April 2024).
[41] E. Rodrigues, M.S. Fernandes, D. Carvalho, Future weather generator for building performance research: an open-source morphing tool and an application, Build. Environ. 233 (2023) 110104, https://doi.org/10.1016/j.buildenv.2023.110104.
[42] R. Fathipour, A. Hadidi, Analytical solution for the study of time lag and decrement factor for building walls in climate of Iran, Energy 134 (2017) 167–180, https://doi.org/10.1016/j.energy.2017.06.009.
[43] S.E. Sadati, N. Rahbar, H. Kargarsharifabad, Energy assessment, economic analysis, and environmental study of an Iranian building: the effect of wall materials and climatic conditions, Sustain. Energy Technol. Assessments 56 (2023), https://doi.org/10.1016/j.seta.2023.103093.
[44] World Health Organization and the United Nations Framework Convention on Climate Change, Iran (Islamic Republic of) Health and Climate Change Country Profile 2022, 2022.
[45] B. Rosti, A. Omidvar, N. Monghasemi, Optimal insulation thickness of common classic and modern exterior walls in different climate zones of Iran, J. Build. Eng. 27 (2020) 100954, https://doi.org/10.1016/j.jobe.2019.100954.
[46] S. Zahiri, H. Altan, Improving energy efficiency of school buildings during winter season using passive design strategies, Sustain. Build 5 (2020) 1, https://doi.org/10.1051/sbuild/2019005.
[47] M. Mehravar, A. Veshkini, S. Veiseh, R. Fayaz, Physical properties of straw bale and its effect on building energy conservation and carbon emissions in different climatic regions of Iran, Energy Build. 254 (2022), https://doi.org/10.1016/j.enbuild.2021.111559.
[48] G. Roshan, R. Oji, S. Attia, Projecting the impact of climate change on design recommendations for residential buildings in Iran, Build. Environ. 155 (2019) 283–297, https://doi.org/10.1016/j.buildenv.2019.03.053.
[49] E. Rodrigues, N. Azimi Fereidani, M.S. Fernandes, A.R. Gaspar, Climate change and ideal thermal transmittance of residential buildings in Iran, J. Build. Eng. 74 (2023) 106919, https://doi.org/10.1016/j.jobe.2023.106919.
[50] Climate.OneBuilding, Org – Repository of Free Climate Data for Building Performance Simulation, 2021. http://climate.onebuilding.org/default.html. (Accessed 27 May 2021).
[51] ISO 15927-4:2005 Hygrothermal performance of buildings – calculation and presentation of climatic data. https://www.iso.org/standard/41371.html, 2005.
[52] E. Rodrigues, D. Carvalho, M.S. Fernandes, Future Weather Generator – morphs current weather for performance simulation of buildings in the future. http://adai.pt/future-weather-generator/, 2022. (Accessed 9 January 2023).
[53] R. Döscher, M. Acosta, A. Alessandri, P. Anthoni, T. Arsouze, T. Bergman, R. Bernardello, S. Boussetta, L.-P. Caron, G. Carver, M. Castrillo, F. Catalano, I. Cvijanovic, P. Davini, E. Dekker, F.J. Doblas-Reyes, D. Docquier, P. Echevarria, U. Fladrich, R. Fuentes-Franco, M. Gröger, J.v. Hardenberg, J. Hieronymus, M. P. Karami, J.-P. Keskinen, T. Koenigk, R. Makkonen, F. Massonnet, M. Ménégoz, P. A. Miller, E. Moreno-Chamarro, L. Nieradzik, T. van Noije, P. Nolan, D. O'Donnell, P. Ollinaho, G. van den Oord, P. Ortega, O.T. Prims, A. Ramos, T. Reerink, C. Rousset, Y. Ruprich-Robert, P. Le Sager, T. Schmith, R. Schrödner, F. Serva, V. Sicardi, M. Sloth Madsen, B. Smith, T. Tian, E. Tourigny, P. Uotila, M. Vancoppenolle, S. Wang, D. Wårlind, U. Willén, K. Wyser, S. Yang, X. Yepes-Arbós, Q. Zhang, The EC-earth3 earth system model for the coupled model Intercomparison project 6, Geosci. Model Dev. (GMD) 15 (2022) 2973–3020, https://doi.org/10.5194/gmd-15-2973-2022.
[54] CMIP6 – coupled model Intercomparison project Phase 6. https://pcmdi.llnl.gov/CMIP6/, 2019. (Accessed 22 March 2024).
[55] R. Haarsma, M. Acosta, R. Bakhshi, P.-A. Bretonnière, L.-P. Caron, M. Castrillo, S. Corti, P. Davini, E. Exarchou, F. Fabiano, U. Fladrich, R. Fuentes Franco, J. García-Serrano, J. von Hardenberg, T. Koenigk, X. Levine, V.L. Meccia, T. van Noije, G. van den Oord, F.M. Palmeiro, M. Rodrigo, Y. Ruprich-Robert, P. Le Sager, E. Tourigny, S. Wang, M. van Weele, K. Wyser, HighResMIP versions of EC-Earth: EC-Earth3P and EC-Earth3P-HR – description, model computational performance and basic validation, Geosci. Model Dev. (GMD) 13 (2020) 3507–3527, https://doi.org/10.5194/gmd-13-3507-2020.
[56] W. Hazeleger, X. Wang, C. Severijns, S. Ştefănescu, R. Bintanja, A. Sterl, K. Wyser, T. Semmler, S. Yang, B. van den Hurk, T. van Noije, E. van der Linden, K. van der Wiel, EC-Earth V2.2: description and validation of a new seamless earth system prediction model, Clim. Dyn. 39 (2012) 2611–2629, https://doi.org/10.1007/s00382-011-1228-5.
[57] B.C. O'Neill, C. Tebaldi, D.P. van Vuuren, V. Eyring, P. Friedlingstein, G. Hurtt, R. Knutti, E. Kriegler, J.-F. Lamarque, J. Lowe, G.A. Meehl, R. Moss, K. Riahi, B. M. Sanderson, The scenario model Intercomparison project (ScenarioMIP) for CMIP6, Geosci. Model Dev. (GMD) 9 (2016) 3461–3482, https://doi.org/10.5194/gmd-9-3461-2016.
[58] E. Rodrigues, M.S. Fernandes, D. Carvalho, M.S. Fernandes, Documentation of future weather generator. https://adai.pt/future-weather-generator/documentation/, 2022. (Accessed 30 March 2022).
[59] E. Rodrigues, M.S. Fernandes, Á. Gomes, A.R. Gaspar, J.J. Costa, Performance-based design of multi-story buildings for a sustainable urban environment: a case study, Renew. Sustain. Energy Rev. 113 (2019) 109243, https://doi.org/10.1016/j.rser.2019.109243.
[60] E. Rodrigues, A.R. Gaspar, Á. Gomes, An evolutionary strategy enhanced with a local search technique for the space allocation problem in architecture, Part 1: Methodology, Comput. Des. 45 (2013) 887–897, https://doi.org/10.1016/j.cad.2013.01.001.
[61] E. Rodrigues, A.R. Gaspar, Á. Gomes, An approach to the multi-level space allocation problem in architecture using a hybrid evolutionary technique, Autom. Constr. 35 (2013) 482–498, https://doi.org/10.1016/j.autcon.2013.06.005.
[62] E. Rodrigues, A.R. Gaspar, Á. Gomes, An evolutionary strategy enhanced with a local search technique for the space allocation problem in architecture, Part 2: validation and performance tests, Comput. Des. 45 (2013) 898–910, https://doi.org/10.1016/j.cad.2013.01.003.
[63] E. Rodrigues, A.R. Gaspar, Á. Gomes, Automated approach for design generation and thermal assessment of alternative floor plans, Energy Build. 81 (2014) 170–181, https://doi.org/10.1016/j.enbuild.2014.06.016.
[64] E. Rodrigues, M.S. Fernandes, Overheating risk in Mediterranean residential buildings: comparison of current and future climate scenarios, Appl. Energy 259 (2020) 114110, https://doi.org/10.1016/j.apenergy.2019.114110.
[65] National Building Regulations of Iran, 2019. https://inbr.ir/wp-content/uploads/2016/08/mabhas-19.pdf.
[66] International Energy Agency, The Future of Cooling: Opportunities for Energy-Efficient Air Conditioning, 2018.
[67] A. Levesque, R.C. Pietzcker, L. Baumstark, S. De Stercke, A. Grübler, G. Luderer, How much energy will buildings consume in 2100? A global perspective within a scenario framework, Energy 148 (2018) 514–527, https://doi.org/10.1016/j.energy.2018.01.139.
[68] F. Knobloch, H. Pollitt, U. Chewpreecha, V. Daioglou, J.-F. Mercure, Simulating the deep decarbonisation of residential heating for limiting global warming to 1.5 °C, Energy Effic 12 (2019) 521–550, https://doi.org/10.1007/s12053-018-9710-0.
[69] ISO 13786:2017 – Thermal Performance of Building Components Dynamic Thermal Characteristics: Calculation Methods, International Organization for Standardization, 2017. https://www.iso.org/standard/65711.html.
[70] Census – statistical center of Iran. https://www.amar.org.ir/Portals/0/census/1395/results/tables/maskan/tafsili/shahrestan/1/1-maskan-01-u.xls, 2016. (Accessed 10 April 2024).
[71] C. Kendrick, R. Ogden, X. Wang, B. Baiche, Thermal mass in new build UK housing: a comparison of structural systems in a future weather scenario, Energy Build. 48 (2012) 40–49, https://doi.org/10.1016/j.enbuild.2012.01.009.